ELSEVIER

Quaternary Science Reviews 24 (2005) 1391–1411

QSR

Climatic and topographic controls on the style and timing of Late Quaternary glaciation throughout Tibet and the Himalaya defined by ^{10}Be cosmogenic radionuclide surface exposure dating

Lewis A. Owen[a,*], Robert C. Finkel[b], Patrick L. Barnard[c], Ma Haizhou[d], Katsuhiko Asahi[e], Marc W. Caffee[f], Edward Derbyshire[g]

[a]*Department of Geology, University of Cincinnati, Cincinnati, OH 45221-0013, USA*
[b]*Lawrence Livermore National Laboratory, Center for Accelerator Mass Spectrometry, Livermore, CA 94550, USA*
[c]*United States Geological Survey, Pacific Science Center, 400 Natural Bridges Drive, Santa Cruz, CA 95060, USA*
[d]*Institute of Saline Lakes, Chinese Academy of Sciences, Xining, Qinghai, PR China*
[e]*Department of Geography, Tokyo Metropolitan University, Tokyo, 192-0397, Japan*
[f]*Department of Physics/PRIME Lab., Purdue University, West Lafayette, IN 47907, USA*
[g]*Centre for Quaternary Research, Department of Geography, Royal Holloway, University of London, Egham, Surrey, TW20 0EX, UK*

Received 25 June 2003; accepted 24 October 2004

Abstract

Temporal and spatial changes in glacier cover throughout the Late Quaternary in Tibet and the bordering mountains are poorly defined because of the inaccessibility and vastness of the region, and the lack of numerical dating. To help reconstruct the timing and extent of glaciation throughout Tibet and the bordering mountains, we use geomorphic mapping and ^{10}Be cosmogenic radionuclide (CRN) surface dating in study areas in southeastern (Gonga Shan), southern (Karola Pass) and central (Western Nyainqentanggulha Shan and Tanggula Shan) Tibet, and we compare these with recently determined numerical chronologies in other parts of the plateau and its borderlands. Each of the study regions receives its precipitation mainly during the south Asian summer monsoon when it falls as snow at high altitudes. Gonga Shan receives the most precipitation ($>2000\,\mathrm{mm\,a^{-1}}$) while, near the margins of monsoon influence, the Karola Pass receives moderate amounts of precipitation (500–600 $\mathrm{mm\,a^{-1}}$) and, in the interior of the plateau, little precipitation falls on the western Nyainqentanggulha Shan ($\sim$300 $\mathrm{mm\,a^{-1}}$) and the Tanggula Shan (400–700 $\mathrm{mm\,a^{-1}}$). The higher precipitation values for the Tanggula Shan are due to strong orographic effects. In each region, at least three sets of moraines and associated landforms are preserved, providing evidence for multiple glaciations. The ^{10}Be CRN surface exposure dating shows that the formation of moraines in Gonga Shan occurred during the early–mid Holocene, Neoglacial and Little Ice Age, on the Karola Pass during the Lateglacial, Early Holocene and Neoglacial, in the Nyainqentanggulha Shan date during the early part of the last glacial cycle, global Last Glacial Maximum and Lateglacial, and on the Tanggula Shan during the penultimate glacial cycle and the early part of the last glacial cycle. The oldest moraine succession in each of these regions varies from the early Holocene (Gonga Shan), Lateglacial (Karola Pass), early Last Glacial (western Nyainqentanggulha Shan), and penultimate glacial cycle (Tanggula Shan). We believe that the regional patterns and timing of glaciation reflect temporal and spatial variability in the south Asian monsoon and, in particular, in regional precipitation gradients. In zones of greater aridity, the extent of glaciation has become increasingly restricted throughout the Late Quaternary leading to the preservation of old ($\gg$100 ka) glacial landforms. In contrast, in regions that are very strongly influenced by the monsoon ($\gg 1600\,\mathrm{mm\,a^{-1}}$), the preservation potential of pre-Lateglacial moraine successions is generally extremely poor. This is possibly because Lateglacial and Holocene glacial advances may have been more extensive than early glaciations and hence may have destroyed any landform or sedimentary evidence of earlier glaciations. Furthermore, the intense denudation, mainly by fluvial and mass movement processes, which characterize these wetter environments, results in rapid erosion and re-sedimentation of glacial and associated landforms, which also contributes to their poor preservation potential.

*Corresponding author. Tel.: +1 512 556 3732; fax: +1 513 556 6931.
E-mail address: lewis.owen@uc.edu (L.A. Owen).

0277-3791/$ - see front matter © 2004 Elsevier Ltd. All rights reserved.
doi:10.1016/j.quascirev.2004.10.014

1. Introduction

The timing and extent of late Quaternary glaciation throughout the high mountains of Tibet and the Himalaya has attracted much attention during recent years (Owen and Lehmkuhl, 2000; Owen and Zhou, 2002; Owen et al., 2002d; Böse et al., 2003). The Tibetan Plateau has a profound influence on regional and global atmospheric circulation and is therefore important for understanding the dynamics of global environmental change (Ruddiman and Kutzbach, 1989; Molnar and England, 1990; Prell and Kutzbach, 1992; Owen et al., 2002d). In particular, it is becoming increasingly apparent that changes in glaciation and snow cover on both short (years to decades) and long (thousands of years) timescales have a profound affect on the regional climate, glaciation and hydrological regimes (Hahn and Shukla, 1976; Dey and Bhanu Khumar, 1982; Dey et al., 1985; Dickson, 1984; Sirocko et al., 1991; Prell and Kutzbach, 1992; Soman and Slingo, 1997; Bush, 2000, 2002; Zhao and Moore, 2004).

Two major climatic systems, the mid-latitude westerlies and the south Asian monsoon, dominate the climatology of the Tibetan Plateau and the Himalaya (Figs. 1 and 2). In addition, the El Niño Southern Oscillation (ENSO) produces significant inter-annual climatic variability in the region. Benn and Owen (1998) highlighted the importance of these climatic systems on glacier formation both regionally and on local scales, and suggested that the relative importance of each climatic system varied throughout the Quaternary, in turn influencing the style and timing of glaciation throughout the region. They noted that the affect of the monsoon is greatest on the eastern and southern slopes of the Himalaya and in eastern Tibet, all of which experience a pronounced summer maximum in precipitation that falls as snow at high altitudes as the result of moisture advection northwards from the Indian Ocean. This summer precipitation, however, declines sharply from south to north across the main Himalayan chain and is also much higher at the eastern end of the mountain belt than in the west. In contrast, the more northern and western ranges, such as the Karakoram Mountains and the western Kunlun, in NW Tibet, receive heavy snowfall during the winter supplied by the mid-latitude westerlies that draw moisture from the Mediterranean, Black and Caspian Seas. In the extreme west this effect leads to a winter precipitation maximum. Changing lapse rates, related to a reduction in the moisture content of air masses as they are forced over the Himalaya, are also important in determining the variability of snow and ice accumulation across the Himalaya and Tibet. There are also strong

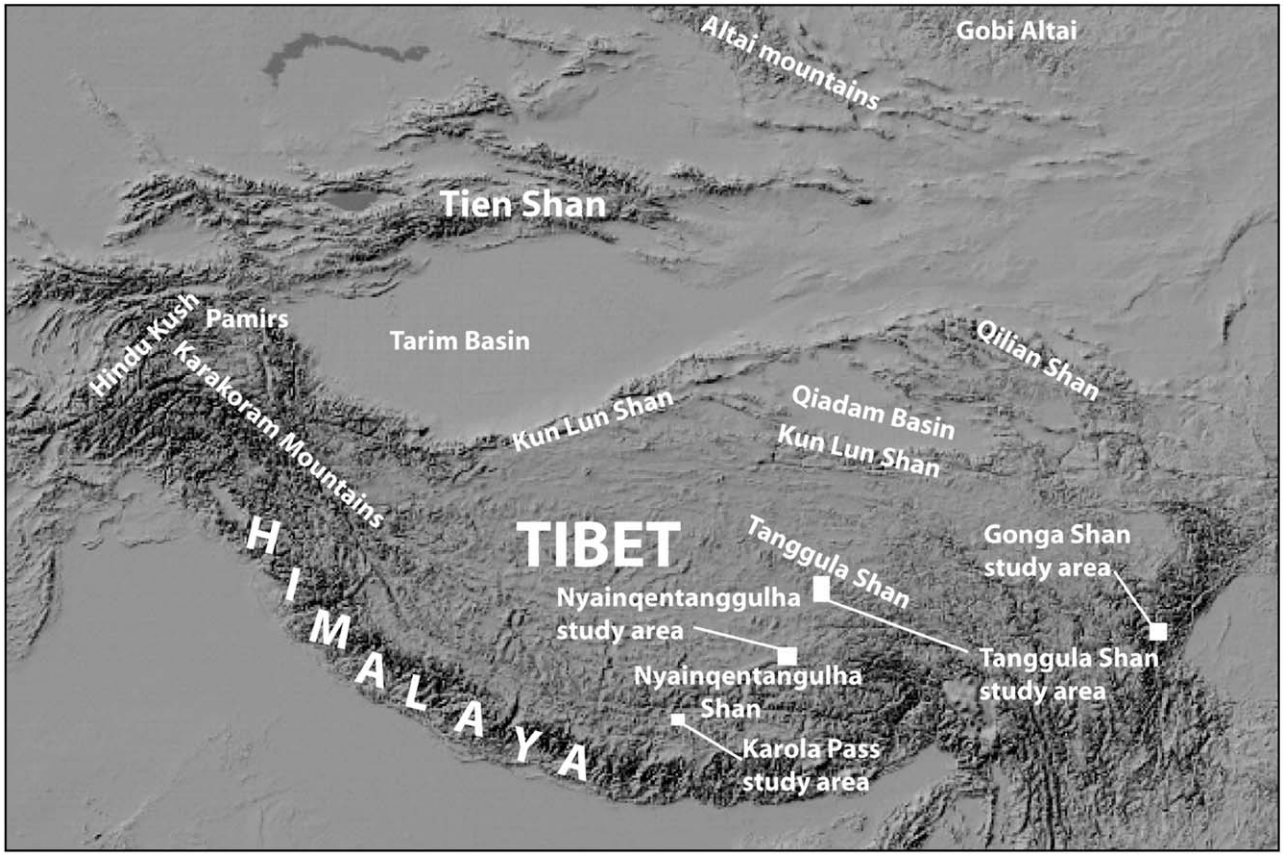

Fig. 1. Digital elevation model of Tibet and the bordering mountains showing the locations of the main study areas.

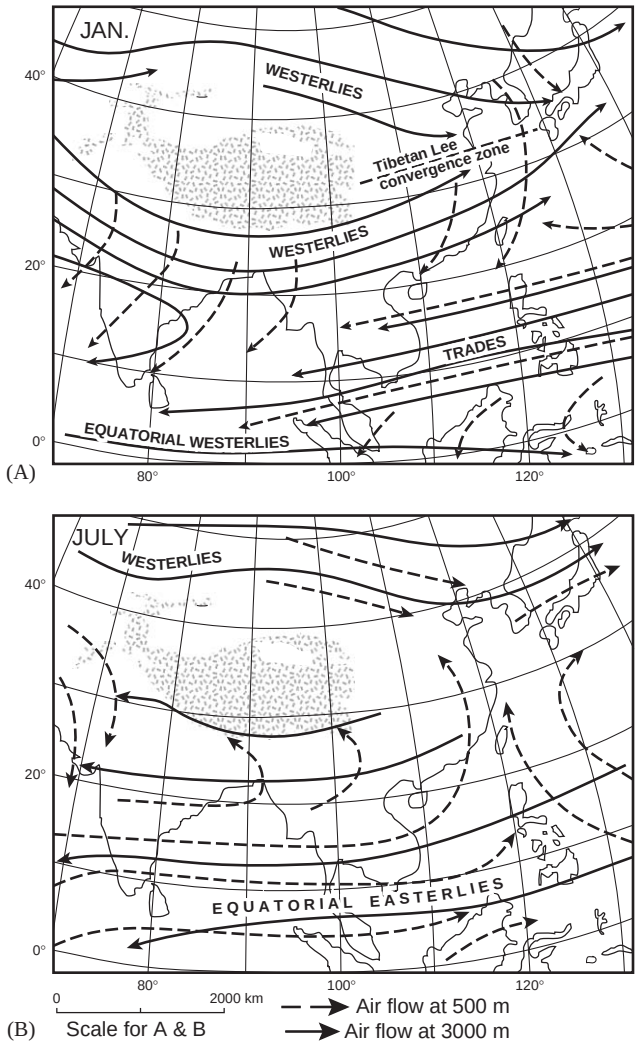

Fig. 2. Summary maps showing the main air flows associated with (A) the south Asian winter and summer (B) monsoons in central Asia. Adapted from Benn and Owen (1998).

microclimatic variations within individual watersheds and also regionally as a result of orographic effects. As climate changed throughout the Quaternary, the relative importance of these climatic systems changed. Benn and Owen (1998) hypothesized that, as a result, Quaternary glaciation may have been asynchronous between different regions of Tibet and the Himalaya. The limited numerical dating control on glacial successions throughout the Himalayan and Tibet did not, however, allow this hypothesis to be tested.

The scarcity of numerical dates is the direct result of the low abundance of organic matter within sediments in these high mountain environments that provided few opportunities for radiocarbon dating. Furthermore, most organic matter present is only of Holocene age (Lehmkuhl, 1997). The development of cosmogenic radionuclide (CRN) and cosmogenic stable nuclides (CSN) surface exposure, and optically stimulated luminescence (OSL) dating, however, has recently allowed the age of previously undateable glacial and associated landforms to be assessed. This has led to the emergence of a framework for the timing of glaciation throughout selected areas of the Himalaya and Tibet (Shiraiwa, 1993; Sharma and Owen, 1996; Phillips et al., 2000; Richards et al., 2000a,b; Owen et al., 2001, 2002a,c, 2003a,b,c, submitted; Schäfer et al., 2001; Tsukamoto et al., 2002; Finkel et al., 2003; Zech et al., 2003; Barnard et al., 2004a,b, submitted). These studies are providing a basis for testing Benn and Owen's (1998) hypothesis, and indicate that precipitation changes related to oscillations in the South Asian monsoon were important in controlling glacier fluctuations over at least the last glacial cycle (Richards et al., 2000a,b; Owen et al., 2001, 2002a,b,c, 2003a,b,c; Finkel et al., 2003; Barnard et al., 2004a,b). Furthermore, these results indicate that, although glaciation throughout these regions was broadly synchronous, it was out of phase with fluctuations of the Northern Hemisphere ice sheets and changes in oceanic circulation that predominantly control global climate (Owen et al., 2002a,b; Finkel et al., 2003).

The studies mentioned above mainly pertain to regions in which glaciation is sustained by monsoonal moisture. Much of Tibet, however, is beyond the influence of the monsoon and is classified as semi-arid to arid; glaciers here are largely influenced by the mid-latitude westerlies. Recent work by Schäfer et al. (2001), Yi et al. (2002) and Owen et al. (submitted), in the Tanggula Shan, Puruogangri and Ladakh, at the extreme margins of monsoon influence, suggests that in these arid regions glaciation during most of the last glacial cycle (since ~60 ka) was very limited in extent. It is therefore likely that glaciers beyond the margins of the monsoon influence behaved differently from the monsoon-affected glaciers throughout the Late Quaternary.

In order to investigate the regional pattern of glaciation and to look for correlations between distant regions within the Himalaya–Tibet region, we have undertaken studies of the Quaternary glacial geology of selected areas of southern, southeastern and central Tibet. Using CRN surface exposure dating, we have defined the timing of glaciation as a means of testing the relative importance of different climatic systems in determining the timing and extent of glaciation throughout the region as a whole. These newly defined chronologies and their correlation with adjacent regions are presented in this paper, and used to examine the various climatic processes that might control glaciation.

2. Methods

2.1. Field methods and sampling for CRN dating

The glacial geologic evidence was examined on either side of the Tanggula Pass (Tanggula Mountains), south

of the Samdainkangsang Mountain along the eastern slopes of the western Nyainqentanggulha Mountains, on the eastern side of Karola Pass in southernmost Tibet, and on the eastern slopes of Gonga Shan in the Daxue Shan of SE Tibet (Fig. 1). Standard geomorphic and sedimentological field techniques (cf. Benn and Owen, 2002) were used to determine the genesis of landforms and to help identify a succession of morphostratigraphically distinct moraines within each region. In this way, appropriate sites for CRN dating were identified within each study area.

Zreda and Phillips (1995), Gosse et al. (1995a,b), Gosse and Phillips (2001), Owen et al. (2001, 2002a), Benn and Owen (2002) and Easterbrook et al. (2003) highlighted some of the limitations of dating moraines using CRN and CSN techniques, and cautioned that local records may be fragmented. Nevertheless, many of these problems can be overcome by obtaining numerous CRN and CSN dates on individual moraines, the approach adopted here in dating the moraine succession in each of the study areas (cf. Putkonen and Swanson, 2003; Easterbrook et al., 2003). Samples for CRN dating were collected by chiseling off ~500 g of rock from the upper surfaces of quartz-rich boulders along moraine crests. Locations were chosen where there was no apparent evidence of exhumation or slope instability. The largest boulders were chosen to help reduce the possibility that boulders may have been covered with snow for significant periods (several months) of the year. To provide a check on the reproducibility of the dating and to check for the possibility of inheritance of CRNs, where possible, several boulders were sampled from each moraine ridge. The degree of weathering and the site conditions for each boulder were recorded. Topographic shielding was determined by measuring the inclination from the boulder site to the top of the surrounding mountain ridges and peaks.

2.2. Laboratory methods for CRN dating

First, the samples were crushed and sieved. Quartz was then separated from the 250–500 μm size fraction using the method of Kohl and Nishiizumi (1992). After addition of Be carrier, Be was separated and purified by ion exchange chromatography and precipitation at pH > 7. The hydroxides were oxidized by ignition in quartz crucibles. BeO was then mixed with Nb metal prior to determination of the $^{10}Be/^{9}Be$ ratios by accelerator mass spectrometry at the Center for Accelerator Mass Spectrometry in the Lawrence Livermore National Laboratory. Isotope ratios were compared to ICN ^{10}Be standards prepared by K. Nishiizumi (pers. comm. 1995).

The measured isotope ratios were converted to CRN concentrations in quartz using the total Be in the samples and the sample weights. Radionuclide concentrations were then converted to zero-erosion exposure ages using sea level high latitude (SLHL) ^{10}Be production rate of 5.2 at/g-quartz/y (Stone, 2000). The Be production rate used is based on a number of independent measurements as discussed by Owen et al. (2001, 2002a). Production rates were scaled to the latitude and elevation of the sampling sites using the star scaling factors of Lal and Peters (1967) and Lal (1991) and an assumed 3% SLHL muon contribution, and were further corrected for changes in the geomagnetic field over time. Details of the calculation are given in Owen et al. (2001, 2002a).

3. Study areas

3.1. Gonga Shan

At 7514 m asl, Gonga Shan (Minya Gongkar in Tibetan) is the highest mountain in China, outside of the Himalaya. It is located on the easternmost edge of the Tibetan Plateau in Sichuan Province (Fig. 1). Thomas (1997) states that the maximum precipitation ($>1900\,mm\,a^{-1}$) along the east slopes occurs at 2900 to 3200 m asl, at far lower altitudes than in other Tibetan mountain ranges. However, other studies suggest that the mean annual precipitation is significantly higher (Kodrau, 1981; Pu et al., 1998). Most of this precipitation falls between May and September during the monsoon season. The mean annual temperature and temperature ranges on the eastern slopes of Gonga Shan at 3000 m asl are 3.9 and 17.2 °C (January to July = −4.5–12.7 °C), respectively (Thomas, 1997). The glaciers are of monsoon maritime type with the basal ice temperature around 0 °C (Derbyshire, 1981; Zheng, 1997; Su and Shi, 2002). These are high activity glaciers with terminal positions extending into forest zones at ~2940 m asl. Pu et al. (1998) note that the mean annual air temperature at the equilibrium-line (at 4970 m asl) on the Hailuoguo glacier is −4.4 °C with an annual precipitation of 3357 mm, and basal ice temperatures between −1.0 and 0 °C.

Zheng (1997) summarizes the glacial geomorphological work undertaken by Chinese scientists during the latter part of the last century. These studies include geomorphic mapping, monitoring of recent glacial retreat and radiocarbon dating of the Hailuoguo glacier on the eastern slopes of Gonga Shan (Fig. 3). A four-fold glacial succession is recognized, which Zheng (1997) believes represents the global Last Glacial Maximum (LGM), early to middle Holocene, Neoglacial and Little Ice Age glacial advances. A moraine platform, ~60–120 m above the present river, considered to represent the LGM advance, extends to ~1850 m in the Hailuoguo valley where it forms a cross-valley ridge (Fig. 4). Zheng (1997) cites radiocarbon dates of

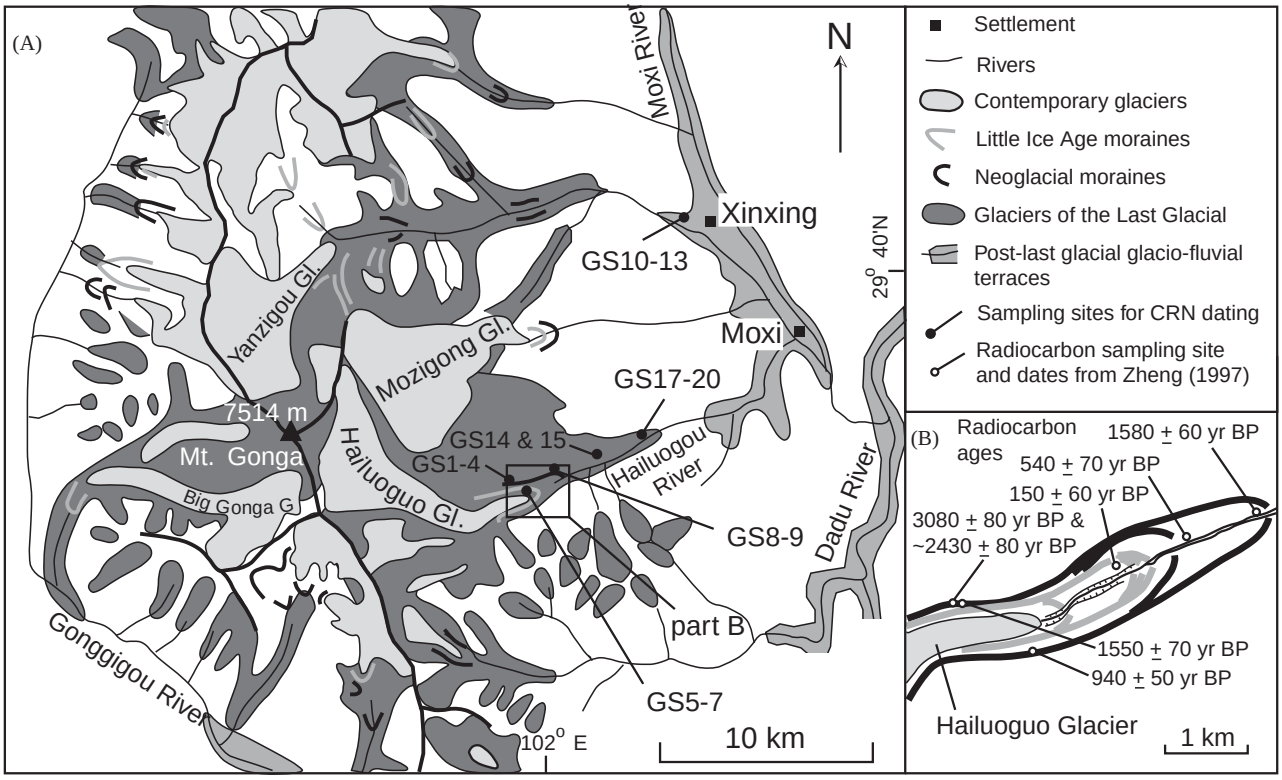

Fig. 3. The Gonga Shan massif showing the main moraines and a reconstruction of the maximum extent of glaciers (A) and the moraines around the Hailuoguo Glacier (B) adapted from Zheng (1997) and the locations for cosmogenic samples. The radiocarbon dates shown in part B are from Zheng (1997).

24,390 ± 750 years BP in silts intercalated within the moraines and 19,700 ± 300 years BP on sinter on the upper moraines. However, no specific details of the dating procedures are provided. Beyond the ice limit, the valley shape changes from broad, typically glacial forms to steep gorge sections. Impressive glaciofluvial terraces (> 50 m thick) are present beyond the limit of Zheng's (1997) LGM moraines and these are considered to be post-last glacial in age (Fig. 5). Zheng expresses the opinion that a lower step in the moraine platform of LGM age represents an early to middle Holocene advance. This is most evident where a ridge dams a small lake at ~2720 m asl on the north side of the Hailuoguo valley ~5 km down valley from the Hailuoguo glacier. He also suggests that this glacial advance is represented by a small end moraine in the upper Moxi valley and in the Gonggigou valley near the confluence of the Ginggigou and Gonga rivers. However, this advance is not marked on the glacial map presented in Zheng (1997). Rather, it is inferred as being within the reconstructed ice extent of the LGM and down valley of the Neoglacial moraines (Fig. 3).

The Neoglacial moraines comprise ridges that rise many tens of metres above the present river level (Fig. 4). Zheng (1997) provides radiocarbon dates of several thousand years for material he describes as 'rotten wood' within the upper parts of the moraines (Fig. 3B). He refers to this advance as the Guanjingtai glacial advance. These moraines extend to within a few kilometres of the present ice margins.

The Little Ice Age moraines form a series of end moraines that rise to several tens of metres above the present river and are inset within the Neoglacial moraines. These extend a few kilometres beyond the present ice margin. A radiocarbon age of 150 ± 60 years is provided for a 'rotten wood' sample from a lateral moraine in front of the Hailuoguo Glacier (Fig. 3).

To test the chronology presented by Zheng (1997), we collected samples from the moraines in the Hailuoguo valley and from the post-Last Glacial glaciofluvial terrace in the Moxi valley (Figs. 3–5). Samples (GS17-20) were collected from Zheng's (1997) terminal position of the LGM in the Hailuoguo valley at ~1860 m asl, while samples GS14 and 15 where collected from the lake dammed by Zheng's (1997) early to middle Holocene moraines at ~2720 m asl (Fig. 3). We also sampled the Neoglacial and Little Ice Age moraines in front of the Hailuoguo Glacier (Figs. 3 and 4).

3.2. Karola Pass

The Karola Pass (sometimes spelt Karila or Karela) at 5042 m asl is the highest road pass on the Lhasa–Yadong Highway. To the north and south lie

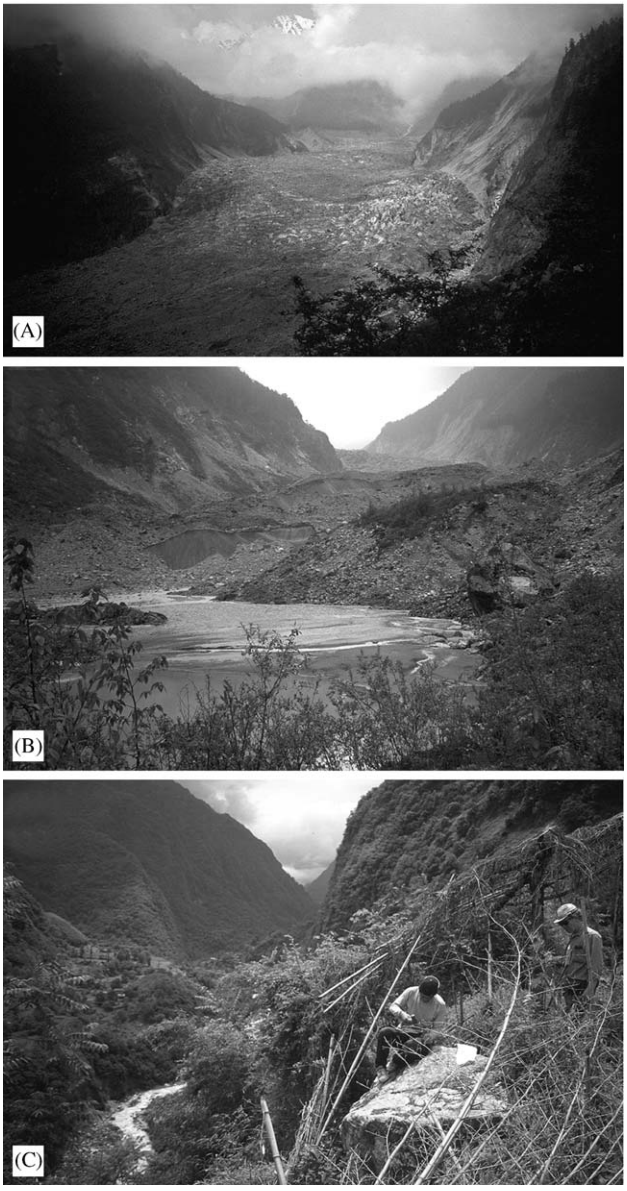

Fig. 4. Views illustrating the characteristics of the geomorphology in the Hailuoguo valley on the eastern slopes of Gonga Shan. (A) Looking west up the Hailuoguo Glacier from the top of Neoglacial moraines. (B) Looking west from the Little Ice Age at the snout of the Hailuoguo Glacier and its historical moraines. (C) View west of a sampling location on the end moraine that marks the maximum extent of glaciation on the eastern slopes of Gonga Shan.

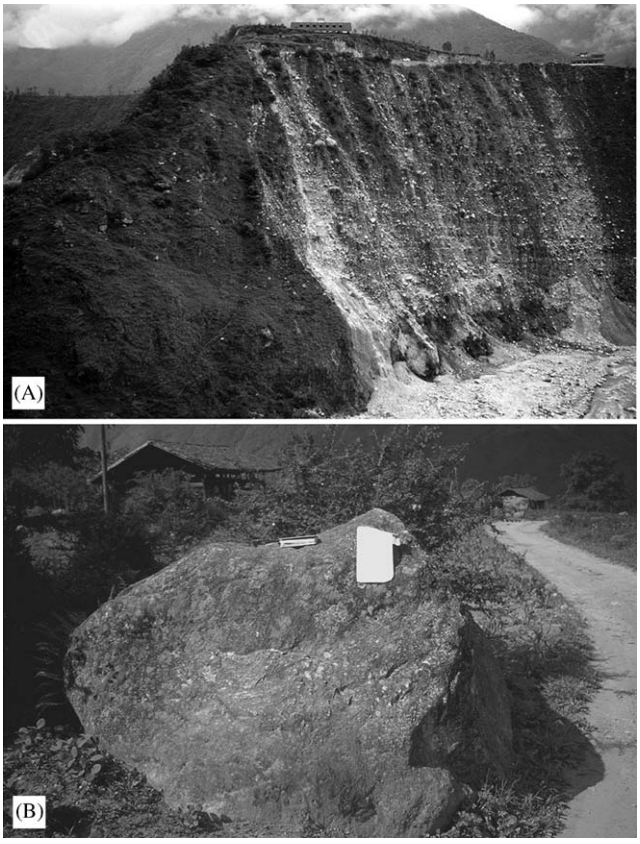

Fig. 5. Exposures within post-Last Glacial glaciofluvial terraces (A) and a typical surface boulder (B) at Xinxing in the Moxi valley east of Gonga Shan. The building in part A and the sampling bag in part B provides a scale. The boulder in part B had large lichens on its surface and was clearly not moved during the construction of the adjacent track.

Mount Lingjing Kangsha (7191 m asl) and Mount Kaluxung (6475 m asl) that are part of southernmost Tibet. The annual precipitation on the pass is ~500–600 mm, most falling as snow during the summer monsoon season. The glaciers in this region are transitional in type between monsoonal and continental (Derbyshire, 1981; Su and Shi, 2002).

Zheng (1989) describes the glacial geomorphology and provides a map of the landforms (Fig. 6). The best succession of moraines is preserved on the west side of the pass, down valley of the Qiangrong glacier. Here the moraines are sharp crested and rise several tens of meters above the valley floor. These are typical of Benn and Owen's (2002) latero-frontal moraines that form on high-altitude debris covered glaciers (Fig. 6B). The oldest moraine, however, comprises denuded till benches that terminate in an end moraine at ~4770 m asl. This is well preserved on the north side of the valley and fluvially cut exposures show that it comprises a well-indurated and sheared deformation till with bullet-shaped clasts in the lower third of the exposure, overlain by a bouldery supraglacial till unit with a more open fabric. Below this moraine, however, the valley retains its broad glaciated form, suggesting an earlier, more extensive glaciation. Zheng (1989) describes till deposits on the north side of the Kaluxung River and west of the Karola Pass as older deposits of the Nieniexongla glaciation. However, we were unable to find the Nieniexongla glacial deposits, described by Zheng (1997), on the east side of the Karola Pass. On the basis of relative weathering criteria, Zheng (1989) believed the moraines to represent glacial advances during the Neoglacial (which they call 'New Glaciation'), Early Holocene

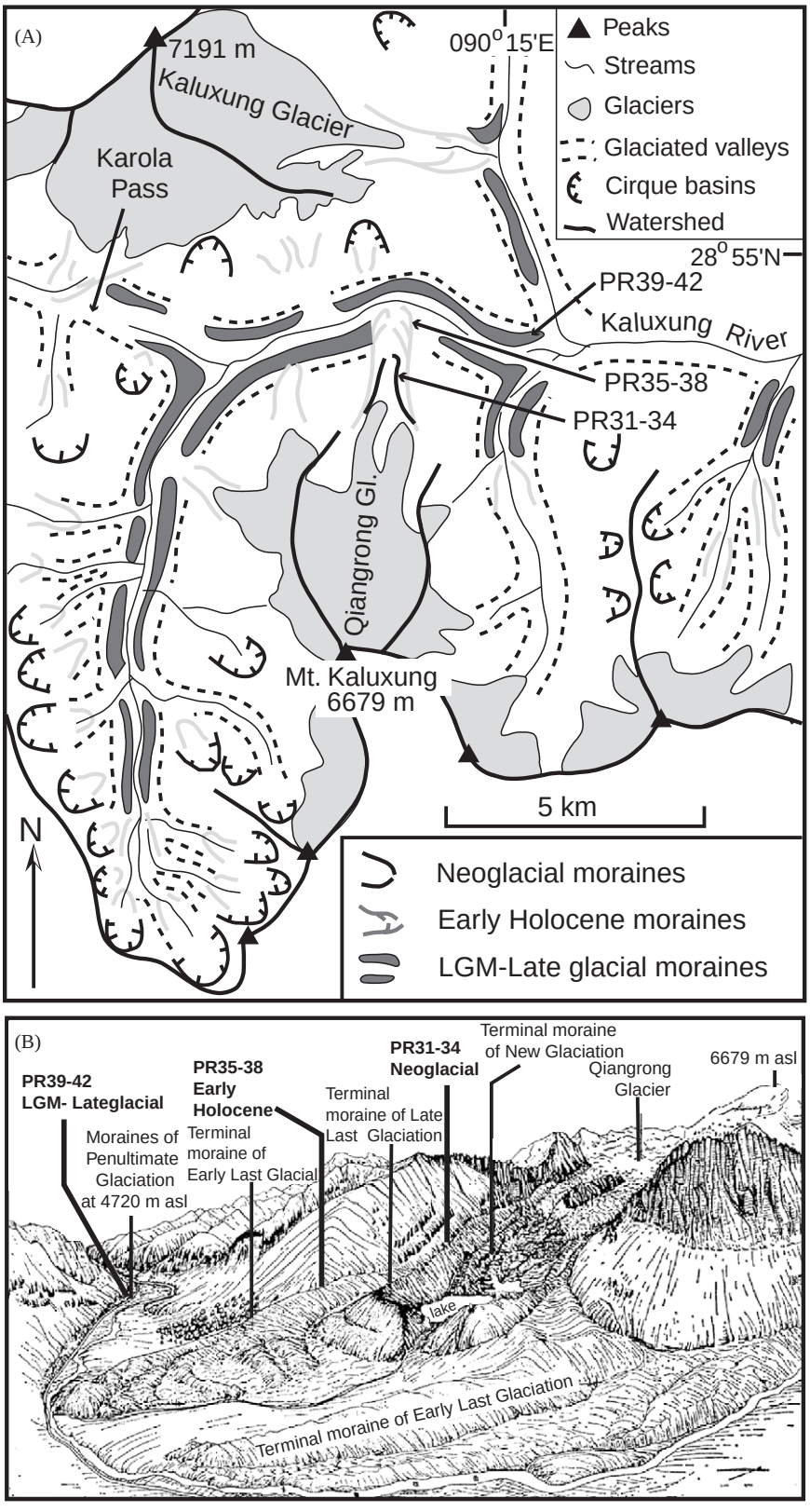

Fig. 6. Geomorphic map (A) and field sketch (B) showing the moraine succession on the Karola Pass showing the sampling locations for CRN dating. The field map is modified from Zheng (1989) and we define the ages of the moraines based on our CRN dating. The field sketch, adapted from Zheng (1989), shows our new interpretation of the moraine ages (in bold text) and Zheng's (1989) interpretation of the moraine ages (in plain text).

Advance, early Last Glacial and penultimate Glacial (Fig. 6B). Samples for CRN dating were collected from each of these moraines (Fig. 6).

3.3. Nyainqentanggulha Shan

The Nyaingentangulha Shan forms an extensive east–west mountain range in southern Tibet to the north of the Tsangpo valley (Fig. 1). This lies on the extreme margin of the present influence of the monsoon, receiving <400 mm precipitation per annum. The glaciers in this region are of cold continental type (Derbyshire, 1981; Su and Shi, 2002).

Lehmkuhl et al. (2002) examined Late Quaternary glacier advances, lake level fluctuations and aeolian sedimentation on the northwestern side of the western Nyainqentanggulha Shan, and suggested evidence for multiple glaciations that spanned the last two glacial cycles. However, they were not able to date the moraines directly in this region. The glacial succession on the more accessible (eastern) side of the western Nyainqentanggulha has not been previously described, despite the presence of well-preserved multiple successions of moraines. At least two major sets of incised lateral-frontal moraines are present within the u-shaped valleys on the eastern side of the western Nyainqentanggulha Shan. Hummocky moraines are present in the forelands of the mountains as much as 5 km from the mountain front. These comprise diamictons containing meter-size boulders (Fig. 8).

For our study area, we chose a valley ~15 km south of Samdainkangsang Peak (6532 m asl), that contained some of the best-preserved moraines, and associated hummocky moraine on the foreland (Figs. 7 and 8). Samples for CRN dating were collected from the hummocky moraine (Fig. 8; samples PR43–47) and from two sets of moraines within the range (Fig. 7; samples PR52–55 and PR48–51).

3.4. Tanggula Shan

The Tanggula Shan is an east–west trending mountain range in central Tibet (Fig. 1). The surrounding lowlands are semi-arid ($\ll 400\,\mathrm{mm\,a^{-1}}$), while the higher peaks of the Tanngula Shan receive up to $\ll 700\,\mathrm{mm\,a^{-1}}$ due to orographic effects during the summer monsoon season. The contemporary glaciers in this region are of cold continental type (Derbyshire, 1981; Pu et al., 1998; Su and Shi, 2002). Pu et al. (1998) showed that, for the Xiao Dongkemadi Glacier in the vicinity of the Tanggula Pass, the mean annual temperature and precipitation at the equilibrium line is $-9.8\,^{\circ}\mathrm{C}$ and 560 mm (at 5600 m asl), respectively, and the basal ice temperature is $-7.5\,^{\circ}\mathrm{C}$.

The glacial geology of the region was originally described by Zheng and Jiao (1991) who produced a

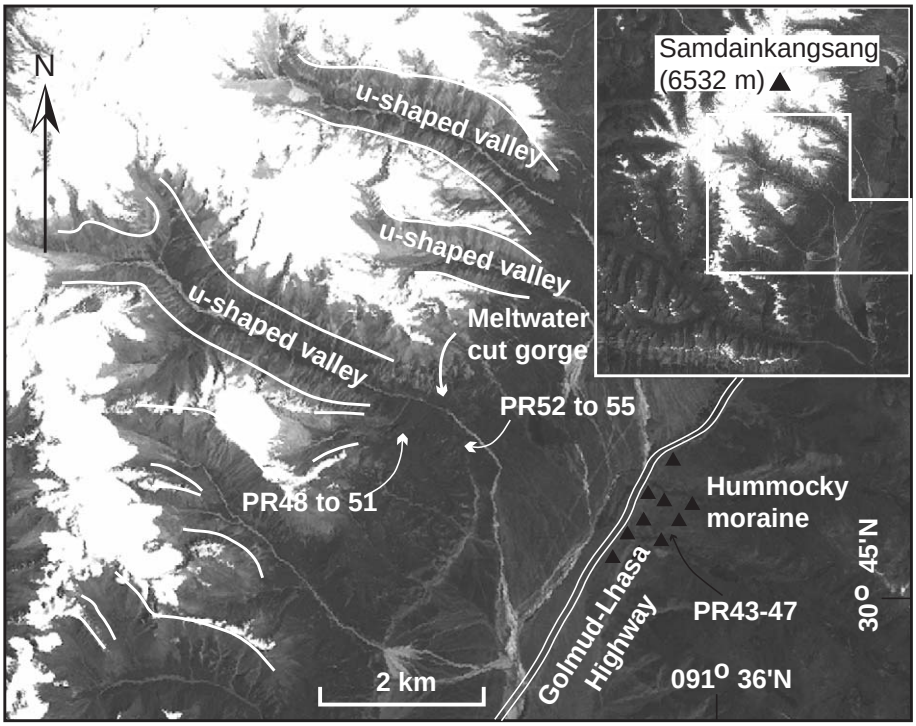

Fig. 7. Geomorphic map of the moraines and associated landforms south of Samdainkangsang Peak on the eastern slopes of the Nyainqentanggulha Shan. The moraines and sampling locations are mapped on a Landsat image.

Fig. 8. View looking southwest at the oldest moraine on the eastern slopes of the Nyainqentanggulha. The boulder in the foreground illustrates a typical sampling location.

map of the Tanggula Pass showing evidence for at least three major glaciations (Fig. 9). They referred to these as the Tanggula Ice Age, the Zhajiazangbo Ice Age and the Bashico Ice Age and regarded them as representing 'extremely old', penultimate, and last glacial cycles, respectively. During the first two of these glaciations, glaciers and ice caps expanded into the forelands from the Tanggula Shan to form a continuous ice cap that, in the area around the Tanggula Pass, was ~90 km and ~25 km wide during the Tanggula and Zhajiazangbo Ice ages, respectively (Derbyshire et al., 1991; Zheng and Jiao, 1991). This produced extensive sheets of till and subdued terminal moraines. The extent of the glacial advance during the Bashico Ice Age was restricted to only several kilometres beyond the present ice margins.

Schäfer et al. (2001) dated four glacial boulders on the Tanggula Pass using ^{10}Be, ^{26}Al, and ^{21}Ne surface exposure dating (Fig. 9). They showed that three boulders within the Tanggula glacial limit had ages of 181.3 ± 15.7, 89.3 ± 8.0 and 172.9 ± 13.8 ka, while a boulder within the limit of the Bashico Ice Age had a surface exposure age of 72.1 ± 6.2 ka. We collected samples from boulders within the same regions as these authors, as well as from moraines dating from the Zhajiazangbo Ice Age. This provides a test of the validity of the glacial ages based on the samples dated by Schäfer et al. (2001), as well as a means of examining the age of the previously undated intermediate glaciation, the Zhajiazangbo.

5. CRN dating results

The ^{10}Be CRN ages determined in this study are listed in Table 1. The ^{10}Be ages are plotted by moraine and relative age in Fig. 10 to show the range and clustering of ages. Such plots provide a qualitative assessment of the potential likelihood of spurious ages due to weathering, exhumation and/or toppling of boulders, and/or derivation of CRN from derived boulders. The CRN dates in Table 1 and Fig. 10, however, have not been corrected for the possibility of weathering. For weathering rates of 1–5 m Ma^{-1}, an exposure age of 10 ka, calculated on the assumption of zero erosion, would underestimate the true age by 1–4%; an age of 20 ka, by 2–9%; an age of 50 ka, by 4–20%; an age of 100 ka, by 10–36%; and an age of 200 ka, by 15–54%. We do not make a correction for shielding due to snow cover because we do not believe it has a significant effect on the ages of our samples. This is because present day snow cover is generally sparse and usually <1 m thick, lasting only a few weeks/months at the elevations from where we collected the samples for dating. Of course snow cover may have been greater during glacial time. However, if snow cover was an important shielding factor in our study areas we would expect to see older ages on the higher boulders on each dated landform. This is because the taller boulders would have had less snow on them than the shorter ones. There is no such relationship between boulder height and age in our data (Table 1) and we therefore conclude that snow cover shielding is not a significant shielding factor in our study areas.

For each of the study areas, the CRN ages on sampled moraines confirm the morphostratigraphy; that is, the sets of ages are progressively younger for morphostratigraphically younger moraines. Furthermore, the dates from most moraines cluster reasonably well. The most notable exceptions are for the Tanggula Shan where the boulder ages are the oldest of all the study areas (Fig. 10D). For example, the moraines of the Zhajiazangbo glacial are well bracketed between the Tanggula and Bashico Glacial Stages at 148 ± 36 ka (mean age and the errors are quoted as 1σ for all the samples dated of the same glacial stage) and 68 ± 26 ka, yet the CRN ages range from >210 to <50 ka (118 ± 73 ka). The young ages may be attributed to extreme weathering (although care was taken to avoid any boulder that showed signs of significant weathering) or recent exhumation by erosion and/or frost heaving. The old ages may be boulders derived from older glacial events and/or ones that were not adequately eroded by glacial processes and therefore have inherited CRNs from prior exposure on hill slopes. Despite the scatter of ages, the data show that the Zhajiazangbo glaciation must have occurred during the early part of the last glacial cycle, the Tanggula Glacial prior to the last interglacial (the younger dates for samples PR58 and PR77 may well be the results of weathering or exhumation) and the Bashico Glacial probably during marine isotope stage (MIS) 4 or the latter part of MIS 5. These data compare well with the CRN dates determined by Schäfer et al. (2001) for the five boulders in his study (Fig. 9).

The dated successions in the Gonga Shan clearly show that the moraines considered by Zheng (1997) to be equivalent to the global LGM, on the basis of

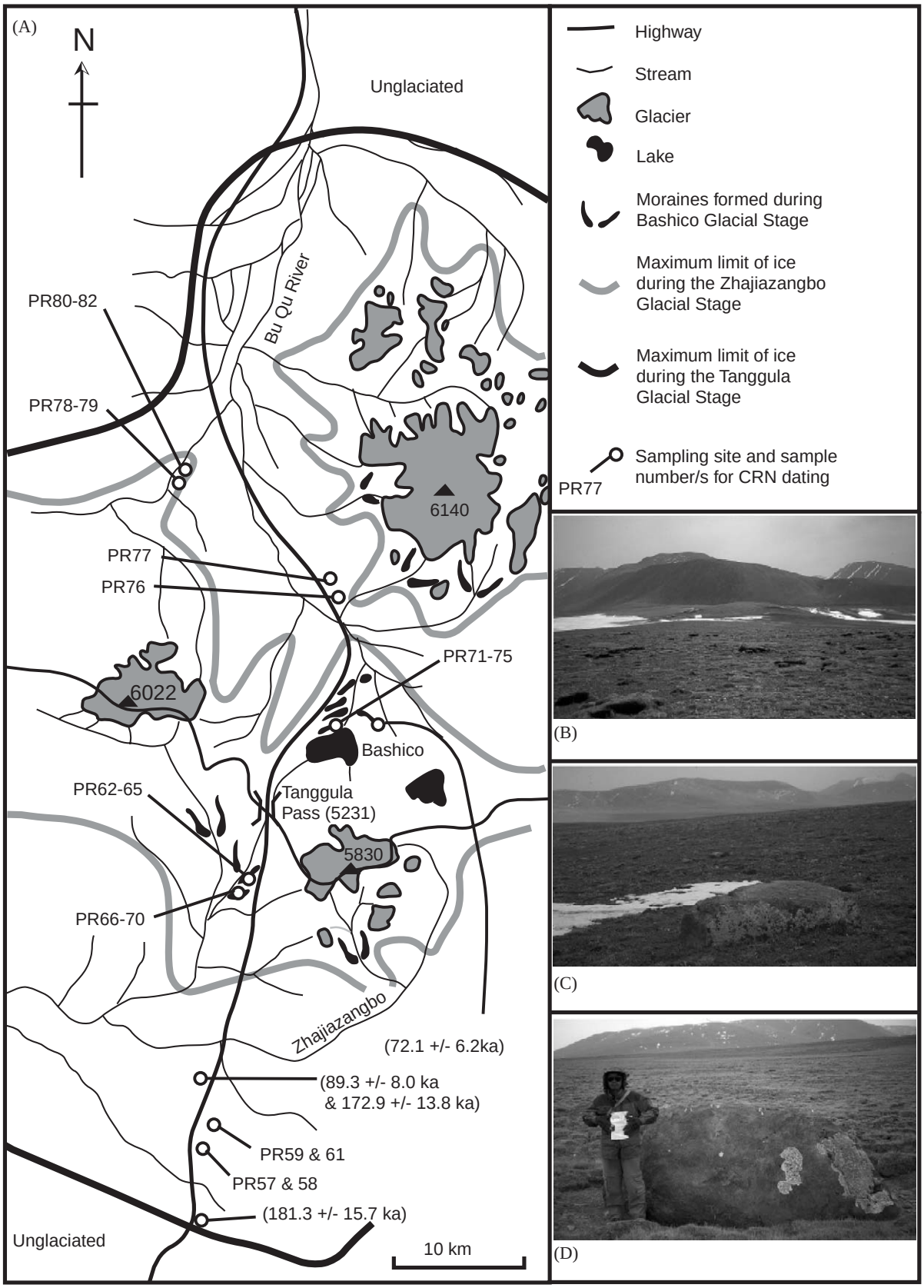

Fig. 9. The glacial geology in the area around the Tanggula Pass. (A) Simplified geomorphic map of the Tanggula Pass showing the sites where we have obtained CRN dates on moraines (modified from Benxing and Keqin, 1991). The dates in parenthesis were undertaken by Schäfer et al. (2001). (B) View of end moraines of the Bashico Glacial Stage south of the Tanggula Pass. (C, D) Typical glacial boulders on surface of moraines deposited during the Zhajiazangbo (C: boulder PR76) and Tanggula Glaciations and (D: boulder PR77).

Table 1
Cosmogenic radionuclide data for Gonga Shan, Karola Pass, Nyainqentanggulha Shan and Tanggula Shan. Samples are grouped per landform in stratigraphic order within each study area

Relative age	Sample	Location latitude/ longitude	Altitude (m asl)	Latitude & altitude correction	Boulder height/ maximum width (m)	10^6 ^{10}Be atoms/ g of quartz	^{10}Be exposure age (ka)
	Gonga Shan						
Youngest moraine	GS5	29°34.277′N/ 101°59.942′E	3010	6.63	1.5/4.5	0.0103±0.0030	0.31±0.09
	GS6	29°34.299′N/ 101°59.935′E	2988	6.54	1.5/3.5	0.0784±0.0295	2.40±0.90
	GS7	29°34.216′N/ 101°59.935′E	2979	6.51	1.2/1.0	0.0121±0.0013	0.37±0.04
	GS1	29°34.191′N/ 101°59.132′E	3174	7.29	2.0/2.0	0.0311±0.0039	0.86±0.11
	GS2	29°34.191′N/ 101°59.132′E	3160	7.23	1.4/1.0	0.0479±0.0061	1.33±0.17
	GS3	29°34.545′N/ 102°00.220′E	3056	6.81	1.0/0.7	0.0246±0.0032	0.72±0.10
	GS4	29°34.545′N/ 102°00.220′E	3056	6.81	1.0/1.0	0.0820±0.0140	2.42±0.41
	GS8	29°34.607′N/ 102°00.186′E	2972	6.48	0.8/1.2	0.0214±0.0101	0.66±0.31
	GS9	29°34.611′N/ 102°00.185′E	2959	6.43	1.2/1.5	0.0271±0.0029	0.85±0.09
Outwash terrace	GS10	29°41.239′N/ 102°04.595′E	2043	3.63	1.1/2.2	0.1129±0.0095	6.25±0.52
	GS11	29°41.233′N/ 102°04.597′E	2110	3.8	1.1/2.5	0.0655±0.0085	3.46±0.45
	GS12	29°41.238′N/ 102°04.617′E	2039	3.62	1.8/4.0	0.1014±0.0083	5.60±0.46
	GS13	29°41.255′N/ 102°04.656′E	2045	3.64	1.8/2.0	0.0592±0.0078	3.27±0.43
	GS14	29°34.145′N/ 102°01.487′E	1670	2.82	0.4/1.2	0.0880±0.0066	6.27±0.47
	GS15	29°35.275′N/ 102°01.267′E	1670	2.82	0.4/1.5	0.0513±0.0079	3.65±0.56
Oldest moraine	GS17	29°36.729′N/ 102°06.208′E	1858	3.21	1.2/1.8	0.1459±0.0080	9.15±0.50
	GS19	29°36.707′N/ 102°06.290′E	1864	3.22	0.5/1.4	0.1352±0.0090	8.43±0.56
	GS20	29°36.707′N/ 102°06.307′E	1884	3.26	1.0/1.4	0.1286±0.0110	7.94±0.68
	GS19R	29°36.707′N/ 102°06.290′E	1864	3.22	0.5/1.4	0.1285±0.0102	7.99±0.64
	GS20R	29°36.690′N/ 102°06.307′E	1884	3.26	1.0/1.4	0.1227±0.0118	7.57±0.73
	Karola Pass						
Youngest moraine	PR31	28°53.439′N/ 090°13.685′E	4980	18.08	0.9/1.2	0.259±0.0238	3.48±0.32
	PR33	28°53.351′N/ 090°13.708′E	4994	18.19	0.3/0.5	0.185±0.0101	2.53±0.13
	PR34	28°53.332′N/ 090°13.711′E	4989	18.15	0.6/1.0	0.167±0.0109	2.09±0.14
	PR35	28°53.680′N/ 090°13.791′E	4914	17.54	0.6/1.0	0.819±0.0247	9.91±3.4
	PR36	28°53.741′N/ 090°13.763′E	4897	17.41	1.7/1.6	0.748±0.0247	9.31±0.31
	PR37	28°53.749′N/ 090°13.756′E	4891	17.36	1.7/2.2	0.856±0.0211	10.63±0.26
	PR38	28°53.758′N/ 090°13.754′E	4878	17.26	0.6/0.6	0.732±0.0177	9.17±0.22

Table 1 (*continued*)

Relative age	Sample	Location latitude/ longitude	Altitude (m asl)	Latitude & altitude correction	Boulder height/ maximum width (m)	10^6 ^{10}Be atoms/ g of quartz	^{10}Be exposure age (ka)
Oldest moraine	PR39	28°53.490′N/ 090°14.985′E	4774	16.45	1.4/2.0	1.16±0.0421	15.65±0.57
	PR40	28°53.498′N/ 090°14.983′E	4781	16.5	0.6/0.7	1.28±0.0465	17.15±0.62
	PR41	28°53.503′N/ 090°14.987′E	4778	16.48	0.3/0.5	1.45±0.0453	19.38±0.61
	PR42	28°53.506′N/ 090°15.014′E	4764	16.37	0.4/0.5	1.17±0.0470	15.83±0.64
	Nyainqentanggulha						
Youngest moraine	PR48	28°46.928′N/ 091°35.387′E	4916	18.45	1.5/4.8	1.44±0.0479	16.79±0.56
	PR49	28°46.927′N/ 091°31.381′E	4919	18.48	1.3/3.8	1.26±0.0366	15.08±0.43
	PR50	28°46.930′N/ 091°31.383′E	4923	18.51	no data	1.24±0.0399	15.67±0.47
	PR51	28°46.928′N/ 091°31.395′E	4922	18.5	0.9/3.0	1.37±0.0417	16.00±0.49
	PR52	28°46.529′N/ 091°32.558′E	4724	16.88	1.1/3.2	1.63±0.0597	20.67±0.76
	PR53	28°46.530′N/ 091°32.558′E	4721	16.85	0.6/2.3	3.537±0.114	41.32±1.33
	PR54	28°46.532′N/ 091°32.571′E	4717	16.82	0.8/2.5	1.54±0.0445	19.60±0.57
	PR55	28°46.523′N/ 091°32.585′E	4712	16.78	1.1/2.1	1.48±0.0408	18.88±0.52
Oldest moraine	PR43	28°46.567′N/ 091°35.917′E	4667	16.43	0.7/1.2	4.31±0.0804	52.62±0.99
	PR44	28°46.538′N/ 091°35.936′E	4669	16.44	0.7/1.5	5.80±0.0929	71.47±1.15
	PR45	28°46.398′N/ 091°35.918′E	4687	16.58	0.6/2.3	8.98±0.219	108.60±2.65
	PR46	28°46.326′N/ 091°35.980′E	4712	16.78	1.4/3.2	4.51±0.102	54.22±1.23
	PR47	28°46.245′N/ 091°36.032′E	4717	16.82	0.5/1.1	4.78±0.107	57.70±1.29
	Tanggula Shan						
Youngest moraine	PR62	32°49.659′N/ 091°54.423′E	5113	20.7	0.4/0.7	5.24±0.135	49.22±1.27
	PR63	32°49.635′N/ 091°54.392′E	5114	21.36	0.4/0.9	5.34±0.0797	50.30±0.75
	PR64	32°49.632′N/ 091°54.394′E	5116	21.37	0.5/0.9	4.88±0.155	45.43±1.44
	PR65	32°49.636′N/ 091°54.390′E	5122	21.39	0.4/0.6	6.48±0.0873	61.85±0.83
	PR66	32°49.220′N/ 091°53.352′E	5067	20.92	0.3/0.8	11.7±0.335	112.71±3.24
	PR67	32°49.240′N/ 091°53.366′E	5071	20.95	0.4/0.7	12.0±0.364	115.80±3.51
	PR68	32°49.245′N/ 091°53.370′E	5068	20.93	0.3/0.5	10.8±0.345	104.70±3.36
	PR69	32°49.203′N/ 091°53.758′E	5099	21.22	0.3/0.5	3.46±0.131	33.85±1.28
	PR70	32°49.207′N/ 091°53.759′E	5100	21.23	0.3/.07	4.94±0.185	46.42±1.74
	PR71	32°56.0.66′N/ 091°58.432′E	5216	22.42	0.3/1.0	5.40±0.227	48.20±2.02
	PR72	32°56.069′N/ 091°58.445′E	5215	22.41	0.2/0.8	7.36±0.240	67.02±2.19
	PR73	32°56.133′N/ 091°58.373′E	5206	22.32	0.8/2.4	7.47±0.186	68.34±1.71

Table 1 (*continued*)

Relative age	Sample	Location latitude/ longitude	Altitude (m asl)	Latitude & altitude correction	Boulder height/ maximum width (m)	10^6 ^{10}Be atoms/ g of quartz	^{10}Be exposure age (ka)
	PR74	32°56.117′N/ 091°58.448′E	5222	22.48	0.4/1.0	6.95±0.319	63.22±2.91
	PR75	32°56.119′N/ 091°58.526′E	5206	22.32	1.0/2.2	8.61±0.471	79.28±4.34
	PR78	33°06.903′N/ 091°50.530′E	4958	20.07	0.7/1.4	2.05±0.267	215.37±2.81
	PR79	33°06.904′N/ 091°50.526′E	4964	20.12	0.3/0.6	12.4±0.376	124.76±3.78
	PR80	33°07.044′N/ 091°50.440′E	4963	20.12	0.6/1.0	4.68±0.242	46.47±2.40
	PR81	33°07.057′N/ 091°50.460′E	4967	20.15	0.7/0.9	4.75±0.211	47.13±2.09
	PR82	33°07.188′N/ 091°50.524′E	4966	20.14	0.4/0.6	15.3±0.732	157.08±7.54
Oldest moraine	PR57	32°38.521′N/ 091°51.563′E	5061	20.76	0.5/1.5	18.0±0.241	181.03±2.43
	PR58	32°38.650′N/ 091°51.728′E	5052	20.68	0.5/1.7	11.0±0.281	107.54±2.76
	PR59	32°38.645′N/ 091°51.739′E	5052	20.68	0.5/1.2	17.7±0.263	178.88±2.66
	PR61	32°38.671′N/ 091°51.714′E	5054	20.69	0.4/1.4	13.9±0.169	136.54±1.66
	PR76	33°00.918′N/ 091°58.059′E	5082	21.17	1.0/3.4	17.7±0.496	175.62±4.91
	PR77	33°01.516′N/ 091°57.698′E	5078	21.14	1.6/3.6	11.0±0.256	105.71±4.39

Atoms of ^{10}Be per gram of quartz before application of shielding correction factor.

radiocarbon dating, have CRN surface exposure ages that are early Holocene (Fig. 10A). The recessional moraine and postglacial glaciofluvial outwash terrace has CRN surface exposure ages indicating that these landforms formed during the middle Holocene (~3–6 ka). Our dating of the Neoglacial and Little Ice Age moraines of Zheng (1997) confirms their Neoglacial (~1–2 ka) and Little Ice Age (a few hundred years) ages.

The difference between the CRN and radiocarbon ages for material indicating the maximum extent of glaciation is difficult to reconcile. The tight clustering of CRN ages suggests that exhumation and weathering of the boulders is unlikely to be the cause of the problem, and that our dates are realistic. It is difficult to assess the validity of the radiocarbon dates because of the lack of specific details presented in Zheng (1997). However, the radiocarbon dates may represent an older moraine that was overridden during an early Holocene glacial advance. Richards et al. (2000a) and Benn and Owen (2002) describe such composite moraines in the Himalaya and provide dates showing that they may form over many millennia and through multiple glacial cycles.

The CRN surface exposure dates for the Karola Pass study area are tightly clustered, showing that the three dated moraines formed at 2.6±0.6, 9.8±0.7 and 17.0±1.7 ka (Fig. 10B). These dates contrast with the chronology suggested by Zheng (1989), which is based on morphostratigraphy and relative weathering criteria. The new data presented here show that the moraine ages should be assigned to the Neoglacial, early Holocene and the global LGM, and not to late Last Glacial, early Last Glacial and the penultimate Glacial as suggested by Zheng (1989; Fig. 6B).

The three sets of moraines on the eastern slopes of the western Nyainqentanggulha Shan have ages that cluster around 69.7±7.8 ka (sample PR45 rejected), 19.7±0.9 ka (sample PR45 rejected) and 15.9±0.9 ka. Samples PR45 and P53 have significantly older ages than the rest of the population and we believe these may be due to inherited CRNs.

6. Discussion

The four research areas considered in this study help illustrate the complexity of the glacial record throughout Tibet. Each of the study areas has a relatively well-preserved succession of moraines representing multiple glaciations. In addition, the extent of glaciation in the

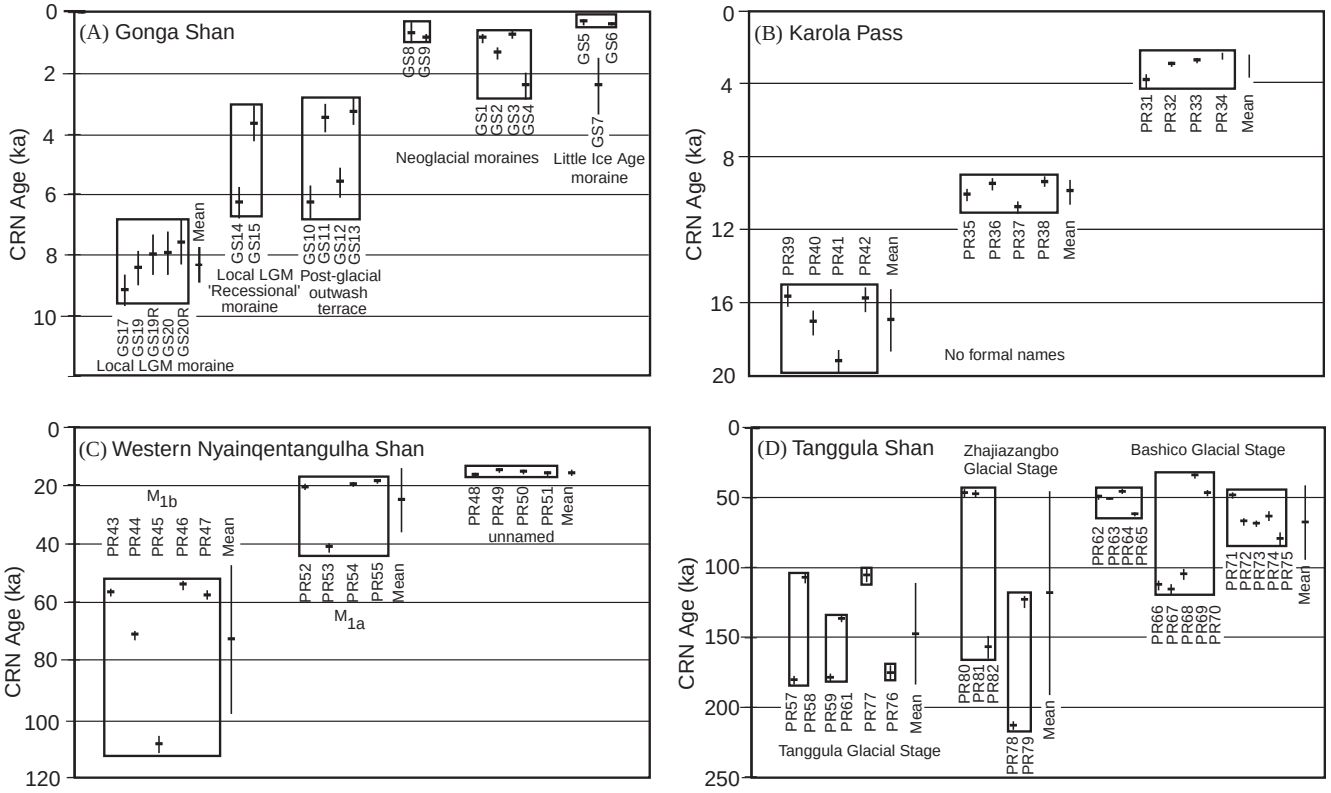

Fig. 10. CRN ^{10}Be surface exposure dates for the moraines dated from each of the study areas. In part A, ^{10}Be CRN surface exposure dates are also presented for the glaciofluvial terraces that were dated in the Moxi valley on the eastern slopes of Gonga Shan. The boxes enclose sets of CRN dates that were collected from the same moraine ridge. The mean values that are shown refer to the mean of the data in the adjacent box and the error bar is expressed as 1σ. Samples GS19R and GS20R are repeat dates of samples GS19 and GS20 from the same boulder.

Gonga Shan, Karola Pass and western Nyainqentanggulha Shan is very similar for each successively older set of moraines. Nevertheless, the ages obtained from these moraines are remarkably different. Furthermore, the moraines in the Tanggula Shan show markedly more extensive glaciations than in the other three study regions and are far older than those in other regions. These observations lead unavoidably to the conclusion that morphostratigraphy and relative dating techniques should only be used with extreme caution when reconstructing regional correlations in the Himalayan–Tibet region. It is understandable, therefore, that moraines such as those on the Karola Pass have been assigned to the wrong glacial ages. Our results highlight the need for intensive numerical dating studies in any new research area within the Himalayan–Tibetan region because of the demonstrably strong regional variability.

The new chronologies presented here show that the ages of the deposits of the oldest preserved glacial advance become progressively older as one moves from monsoon-influenced to semi-arid regions of Tibet. Thus, only Holocene moraines are preserved in the wettest regions (Gonga Shan), while the oldest moraine successions occur in the semi-arid regions of central Tibet, namely the Nyainqentanggulha and Tanggula Shan. The Karola Pass is in a transitional zone between the monsoon-influenced and the semi-arid interior. This is reflected in the fact that the oldest moraines in this region are intermediate in age between the other regions.

The difference in the ages of the moraines between these study areas suggests that preservation and/or style of glacial advance differs markedly throughout Tibet. For example, moraines in monsoon-influenced regions are more likely to be eroded by intense fluvial and mass movement processes, while those in semi-arid regions appear to have been subjected to only minor geomorphic modification, mainly consisting of weathering processes.

The fact that usually only 3–5 sets of moraines are generally present within our study areas might be a result of randomness and obliterative overlap as suggested in Gibbons et al.'s (1984) probability model for the survival of moraines in a succession of glacial advances. However, the regional pattern we describe and illustrate in Fig. 11, suggests that successions of moraines within the Himalaya and Tibet are not the result of random preservation. Moreover, preservation potential by itself does not adequately explain the observed pattern because if it did, some evidence of earlier glacial advances, such as valley form and/or

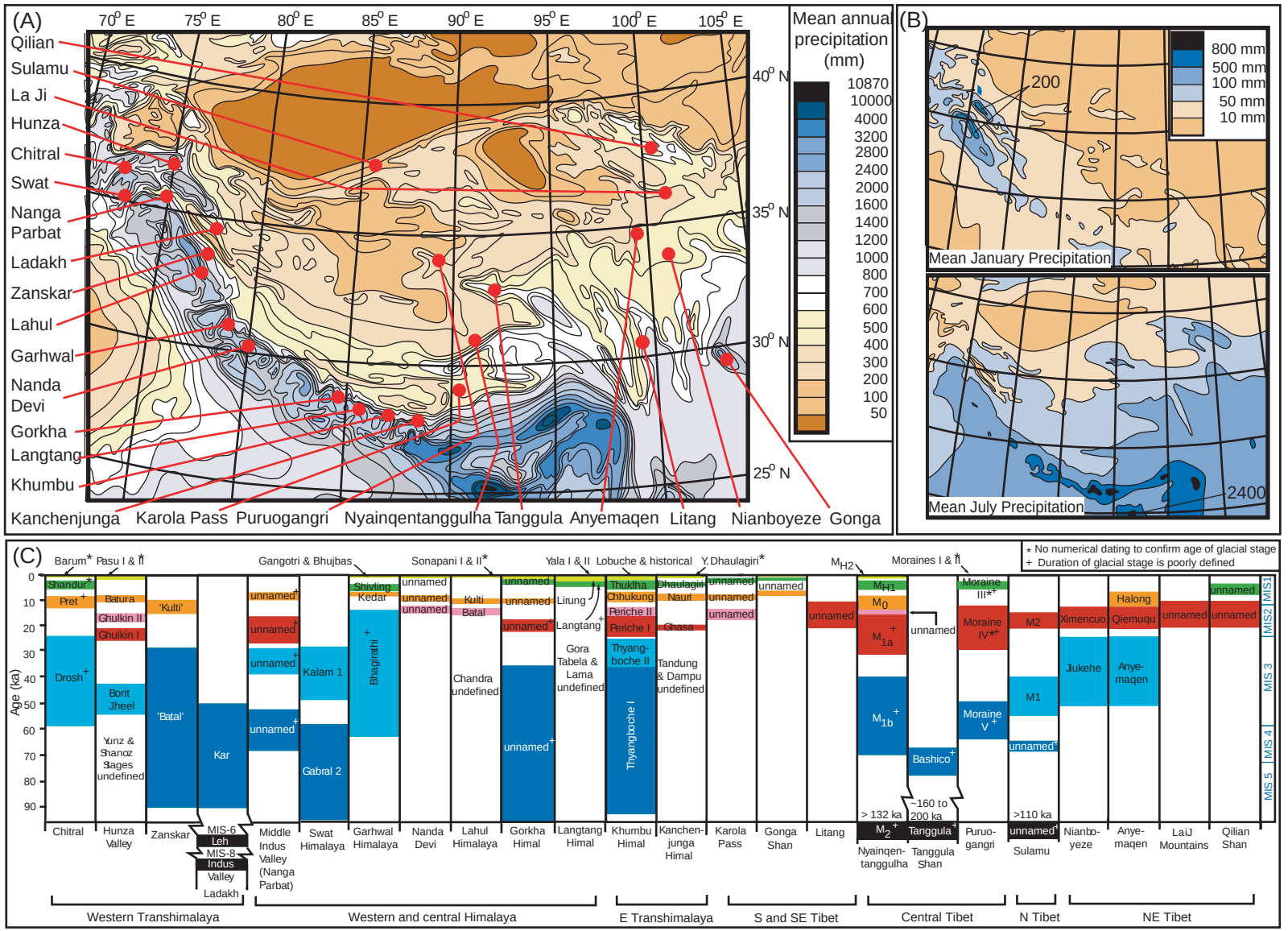

Fig. 11. The contemporary mean annual (A) and mean January and July (B) precipitation across Tibet and the bordering regions showing (C) the locations and glacial chronologies that have been numerically dated throughout the Himalaya and Tibet (data from Shiraiwa, 1993; Sharma and Owen, 1996; Phillips et al., 2000; Richards et al., 2000a,b; Owen et al., 2001, 2002a,c, 2003a,b,c, submitted; Schäfer et al., 2001; Tsukamoto et al., 2002; Yi et al., 2002; Finkel et al., 2003; Zech et al., 2003; Barnard et al., 2004a, unpublished data; Meriaux et al., 2004). The color bars in (C) represents the likely duration of each glacial advance and the name of each glacial stage has been inserted into the box. An asterisk and cross after each name indicates that no numerical dating has been undertaken to confirm an age and the duration of the glacial is poorly defined, respectively. A tentative correlation is suggested by applying similar colors to the bars.

buried tills, should still persist beyond the maximum extent of younger surviving moraines. In Gonga Shan, for example, the valley form changes abruptly from a broad u-shape to a gorged box-shape beyond the early Holocene moraines. This strongly suggests that the early Holocene glacial advances in the monsoon-influenced regions may have been at least as extensive as the Pleistocene glacial advances. This conclusion is consistent with Zheng's (1997) ~20 ka radiocarbon dates from within the moraines dated in this study to the early Holocene if the moraines are composite, produced through the effects of several glacial advances.

Glaciation in the strongly monsoon-influenced Himalaya shows similar patterns to those found in the Gonga Shan. In the wettest monsoon-influenced regions ($>2400\,mm\,a^{-1}$), such as Nanda Devi and Langtang, for example, only Holocene and Lateglacial moraines are present (Barnard et al., 2004b and submitted). In contrast, the driest regions of the Himalaya and Transhimalaya, such as Ladakh, preserve extremely old moraines (>300 ka; Owen et al., submitted). In regions such as the Hunza valley and Khumbu Himal, which are close to the limits of monsoon influence, with annual precipitation in the range of 500–1000 mm, evidence for at least eight glacial advances during the last glacial cycle is preserved, and the maximum extent of glaciation occurred during the early part of the last glacial cycle (Owen et al., 2002a; Finkel et al., 2003). The Karola Pass, which is in a similar transitional zone, is somewhat unusual because it preserves evidence for only four glacial advances (including the Little Ice Age moraines that were not dated in this study) dating back to the global LGM. However, Zheng (1997) cites evidence of older moraines that we were unable to find on the eastern side of the pass. In the Macha Khola valley (Gorkha Himal, Nepal), Zech et al. (2003) showed that moraines formed during MIS 3–4 (or earlier), MIS 2, Lateglacial, mid-Holocene and Late Holocene. The local last glacial maximum occurred during MIS 3–4 (or earlier), but the Macho Khola glacier during MIS 2 was almost the same thickness as it was during MIS 3–4 (or earlier). Zech et al.'s (2003) study adds complexity to our proposed pattern of glaciation because the Gorkha Himal is close to the strongly monsoon-influenced Langtang Himal where only Holocene moraines are preserved. The pattern of moraines in the Macha Khola valley might reflect preservation, but it might also indicate that the climatic conditions in the valley are transitional between the wetter regions of the Langtang and the drier Transhimalaya where evidence for older glaciations is preserved. Given such complexity, we stress the need for more extensive studies of the glacial geology of other areas throughout Tibet and the bordering mountains to test the apparent regional variability in timing and extent of glaciation.

As highlighted by Finkel et al. (2003), glacial advances can be broadly regionally correlated throughout the Himalaya. Our new data presented here, and the data compilation summarized in Fig. 11, suggests this broad regional correlation can be extended across Tibet. It is apparent that glacial advances occurred during the Little Ice Age, Neoglacial, Middle Holocene, early Holocene, Lateglacial Interstadial, ~15 ka (~Heinrich Event 1), global LGM, one/two advances during MIS 3, early Last Glacial and an in earlier glacial cycles. However, each of these glaciations is not represented in every region. In the wettest regions only the Holocene moraines survive. Multiple glaciations on sub-Milankovitch timescales are supported by the ice core work on the Dunde and Guiliya ice caps in NW Tibet (Thompson et al., 1989, 1997). Fig. 12 plots all published ^{10}Be CRN dates for boulders on moraines, including those in this study and compares them with the January and June insolation curves for the last 400 ka. This compilation clearly reveals the greater abundance of young ages (Holocene and particularly late Holocene) that probably reflects the greater preservation of younger moraines. Nevertheless, distinct clusters of ^{10}Be CRN ages are evident, such as during the Neoglacial, Early Holocene and Heinrich Event 1. Clustering of ^{10}Be CRN dates for the global LGM and MIS 3 is less evident, and dates prior to MIS 4 are sparse.

Our new data supports the views of Owen et al. (2002a, 2003c) and Finkel et al. (2003) that glaciation throughout the Himalaya and Eastern Tibet is strongly controlled by precipitation changes related to oscillations in the South Asian monsoonal system combined with cooling that is broadly associated with Heinrich events. Beyond the heavily monsoon-influenced regions (with annual precipitation $\ll 2000$ mm), the local last glacial maximum occurred early in the last glacial cycle. This observation supports the views of Gillespie and Molnar (1995) and Benn and Owen (1998) who suggested that glaciation in the Himalaya and Tibet was asynchronous with the maximum extent of the Northern Hemisphere ice sheets. In particular, it appears that in many regions, such as the Hunza valley, Khumbu Himal and NE Tibet, glaciers reached their maximum extent during the insolation maximum of MIS 3 (cf. Figs. 11 and 12). Using other proxy data, including lake records and palynology, Shi et al. (2001) emphasized the fact that MIS 3 was a time of enhanced monsoon moisture supply to Tibet. Hence, at high altitudes, snowfall would have increased and glaciers expanded. However, a glacial advance during MIS 3 is not recognized in the data for the new study areas discussed here. Rather, the CRN ages cluster at about 70 ka, albeit not very tightly, in the case of the Nyainqentanggulha and Tanggula Shan, suggesting that glaciers may have advanced during the latter part of MIS 5 or even MIS 4. Unfortunately, CRN dating is

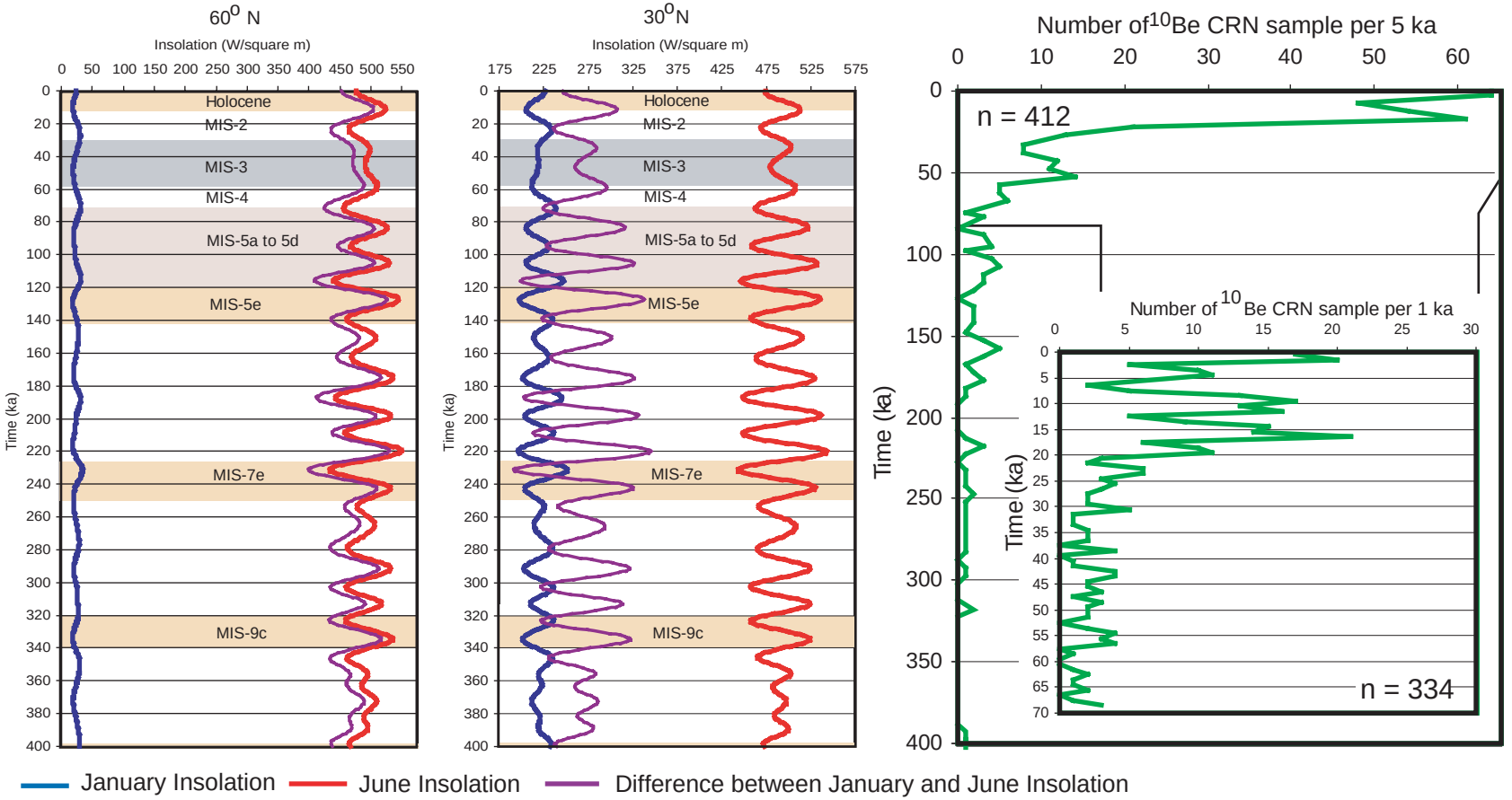

Fig. 12. Insolation curves for 60°N and 30°N for the last 400,000 years (data taken from Berger and Loutre, 1991) compared with the ^{10}Be CRN dates on moraine boulders that have been published for the Himalaya (data from Phillips et al., 2000; Owen et al., 2001, 2002a, 2003a,b,c, submitted; Schäfer et al., 2001; Finkel et al., 2003; Barnard et al., 2004a,b, submitted). The duration of interglacials that are colored light brown are taken from Winograd et al. (1997).

presently not precise enough to allow us to determine whether glaciers advanced in response to increased insolation during MIS 5c or 5a or to cooling during MIS 4, synchronously with the Northern Hemisphere ice sheets. These regions are on the distal margins of monsoon influence and might have responded more readily to changes in the Northern Hemipshere ice sheets and oceans.

Throughout all the regions of the Transhimalaya and Tibet, glacial advances during the global LGM appear to have been very restricted in extent, generally having been limited to <10 km beyond the present ice margins (cf. Owen et al., 2002b). In the Nyainqentanggulha Shan, the LGM advance limit lay within only a few kilometers of the present ice margins, while in the Tanggula Shan it must have been significantly less than the extent of the Bashico Glacial moraines that lie $\sim$10 km from the present ice margin and date from $\sim$70 ka. The restricted advance during this time may have been a consequence of reduced monsoon precipitation during this insolation minimum. During such times, snowfall at high altitudes would be reduced and would severely restrict the ability of glaciers to persist at lower altitudes. On the other hand, temperatures on the Tibetan Plateau lowered by 8–9 °C compared to the present (Shi, 2002) would have made possible some glacier advance to lower altitudes, albeit of limited extent.

The extensive early Holocene advance in the wettest regions and evidence of its presence, albeit moderated, in most of the other study regions through the Himalaya and Tibet (Fig. 11) further support the case for strong monsoonal control. During this insolation maximum (Fig. 12), increased precipitation falling as snow at high altitudes would have produced positive glacier mass balances resulting in glacier advance. The reduced insolation during the winter would have also contributed to the positive glacier mass balance.

Glaciation in the Tanggula Shan was more extensive in the penultimate glacial cycle than during the last glacial cycle. This situation is similar to that observed in other semi-arid regions such as Ladakh and the westernmost Nyainqentangguhla Shan (Owen et al., submitted; Lehmkuhl et al., 2002). Progressive diminution of glacial extent over several glacial cycles is difficult to explain, but might indicate progressive reduction in moisture supply as continued mountain uplift reduced the influence of moisture sources such as the south Asian monsoon and/or the mid-latitude westerlies. Alternatively, this pattern might reflect subtle changes in insolation over individual glacial cycles. For example, summer and winter insolation were higher and lower, respectively, during the penultimate glacial cycle compared to the last glacial cycle at 30°N (Fig. 12). This pattern might have driven more extensive glaciation during the penultimate glacial cycle. However, the insolation values for MIS 8 were not unlike those of the last glacial cycle, yet more extensive glaciations occurred in Ladakh (Owen et al., unpublished data). Therefore, the different patterns of insolation between glacial cycles cannot simply explain the changing styles of glaciation during the last few hundreds of thousands years.

As Schäfer et al. (2001) pointed out, the presence of moraines that antedate the last glacial cycle in the Tanggula Shan provides evidence that an extensive ice sheet, as proposed by Kuhle (e.g. 1985, 1988, 1991, and 1995), could not possibility have existed on the Tibetan Plateau during the last glacial cycle. Had such an ice sheet developed, the glacial landforms and associated boulders from earlier glaciations would have been eroded away. Furthermore, Kuhle used the presence of moraines at low altitudes along the margins of the Tibetan Plateau and in the bordering mountains to support his ice sheet proposal. However, many of the moraines used in Kuhle's ice sheet reconstructions occur in the monsoon-influenced regions; many of these are Holocene in age and are a consequence of high moisture flux delivered by the south Asian summer monsoon to the high mountains that border the Tibetan Plateau.

In summary, there is a general synchroneity in the timing of glaciation in the monsoon-influenced regions of the Himalaya and Tibet, but within the semi-arid regions beyond monsoon influence, glacial advances may be asynchronous, moving in synchrony with the Northern hemisphere ice sheets, possibly under the influence the mid-latitude westerlies. Strong regional variations in the extent of glaciation occur throughout the region. Such variations in extent have yet to be systematically quantified by such techniques as reconstruction of equilibrium-line altitudes (ELAs). However, as Benn and Lehmkuhl (2000), Owen and Benn (2005) and Benn et al. (2005) emphasize, reconstructions of former ELAs in high altitude environments are rife with problems owing to thick supraglacial debris cover, and extreme microclimatic and topographic variability within individual regions. Regional correlations can be adequately achieved only by detailed numerical dating studies within individual areas because, given the strong topographic and climatic gradients, severe errors can arise if only morphostratigraphic correlation and relative weathering studies are relied on. Furthermore, the precision and accuracy of CRN and CSN surface exposure dating is not good enough at present to test the synchronuity of glacial events on sub-millennial scales for the Holocene and Lateglacial, and on sub-Milankovitch scales for pre-LGM times. Improvements in methodologies and further dating studies promise to refine the hypotheses and conclusions presented in our study.

Reconstructions of the timing and extent of Late Pleistocene glaciers in Tibet and the Himalaya are fundamental for improved understanding of the links between climate change, glaciation and hydrology. Recent model results suggest that anthropogenic forcing (e.g. greenhouse gas, land-cover change) is important in controlling variations in the Asian monsoon (Wake et al., 2001), which, in turn, affects glaciation and surface hydrology, changes which could have profound affects on large human populations. While, the variation in glacial style shown in this study adds to the complexity involved in modeling and predicting future glacial and hydrological change, it does provide a working framework with which to begin the process of examining more closely the connections between atmosphere, cryosphere and hydrosphere in the high mountains of central Asia.

7. Conclusions

The style and timing of glaciation in regions of contrasting climate across the Tibetan Plateau are defined using geomorphic techniques and CRN dating. In each of the study areas, the sets of preserved and dated moraines show that Quaternary glaciation became progressively less extensive with time. In the Gonga Shan, the moraines date from the early mid Holocene, Neoglacial and Little Ice Age. The glacial moraines on the east side of the Karola Pass date from the Lateglacial, Early Holocene and Neoglacial. In contrast, the moraines on the western slopes of the Nyainqentanggulha Shan date from the early part of the last glacial cycle, global LGM and Lateglacial, while the two sets of moraines in the Tanggula Shan date from the penultimate glacial cycle and the early part of the last glacial cycle. We believe that the regional patterns and timing of glaciation throughout Tibet reflect temporal and spatial variability in the south Asian monsoon and, in particular, regional precipitation gradients. Old moraines are more readily preserved in regions of greater aridity, such as the Tanggula Shan and the Nyainqentanggulha Shan. In contrast, within regions with greater rainfall as a result of the strong influence of the monsoon, the preservation potential of pre-Lateglacial moraine successions is extremely poor because of the associated high erosion rates. Furthermore, we suggest that glaciation in such regions during the early Holocene insolation maximum was probably more extensive than earlier in the last glacial cycle (and specifically at the global LGM), and thus any evidence of older moraines would have been destroyed by subsequent glacial advances. However, this hypothesis needs to be tested in future studies of the glacial geology and/or using other proxies such as lake records within each of the study areas throughout Tibet and the Himalaya. We therefore believe that glaciation throughout Tibet and the Himalaya is strongly influenced by orography that, in turn, strongly influences climate.

Acknowledgements

We would like to thank the Pacific Rim Program of the University of California for funding our fieldwork. This work was performed under the auspices of the US Department of Energy by the University of California, Lawrence Livermore National Laboratory, under Contract No. W-7405-Eng-48 as part of an IGPP/LLNL research grant. Particular thanks to Douglas Benn and John Gosse for their constructive and helpful reviews of our paper.

References

Barnard, P.L., Owen, L.A., Finkel, R.C., 2004a. Style and timing of glacial and paraglacial sedimentation in a monsoonal influenced high Himalayan environment, the upper Bhagirathi Valley, Garhwal Himalaya. Sedimentary Geology 165, 199–221.

Barnard, P.L., Owen, L.A., Sharma, M.C., Finkel, R.C., 2004b. Late Quaternary landscape evolution of a monsoon-influenced high Himalayan valley, Gori Ganga, Nanda Devi, NE Garhwal. Geomorphology 61, 91–110.

Benn, D.I., Lehmkuhl, F., 2000. Mass balance and equilibrium-line altitudes of glaciers in high mountain environments. Quaternary International 65/66, 15–29.

Benn, D.I., Owen, L.A., 1998. The role of the Indian summer monsoon and the mid-latitude westerlies in Himalayan glaciation: review and speculative discussion. Journal of the Geological Society 155, 353–363.

Benn, D.I., Owen, L.A., 2002. Himalayan glacial sedimentary environments: a framework for reconstructing and dating former glacial extents in high mountain regions. Quaternary International 97–98, 3–26.

Benn, D.I., Owen, L.A., Osmaston, H.A., Seltzer, G.O., Porter, S.C., Mark, B., 2005. Reconstruction of equilibrium-line altitudes for tropical and sub-tropical glaciers. Quaternary International, in press.

Berger, A., Loutre, M.F., 1991. Insolation values for the climate of the last 10 million years. Quaternary Science Reviews 10, 297–317.

Böse, M., Hirakawa, K., Matsuoka, N., Sawagaki, T., 2003 (Eds.), Glaciation and periglaciation in Asian high Mountains. Zeitschrift für Geomorphologie 130, 276pp.

Bush, A.B.G., 2000. A positive climatic feedback mechanism for Himalayan glaciation. Quaternary International 65/66, 3–13.

Bush, A.B.G., 2002. A comparison of simulated monsoon circulations and snow accumulation in Asia during the mid-Holocene and at the Last Glacial Maximum. Global and Planetary Change 32, 331–347.

Derbyshire, E., 1981. Glacier regime and glacial sediment facies: a hypothetical framework for the Qinghai-Xizang Plateau. In: Proceedings of the Symposium on Qinghai-Xizang (Tibet) Plateau, Beijing China. Vol. 2—Geological and Ecological Studies of Qinghai-Xizangf Plateau. Science Press, Beijing, pp. 1649–1656.

Derbyshire, E., Shi, Y., Li, J., Zheng, B., Li, S., Wang, J., 1991. Quaternary glaciation of Tibet: the geological evidence. Quaternary Science Reviews 10, 485–510.

Dey, B., Bhanu Khumar, O.S.R.U., 1982. An apparent relationship between Eurasian spring snow cover and the advance period of the

Indian summer monsoon. Journal of Applied Meteorology 21, 1923–1929.

Dey, B., Kathuria, S.N., Bhanu Khumar, O.S.R.U., 1985. Himalayan snow cover and withdrawal of the Indian summer monsoon. Journal of Climatology and Applied Meteorology 24, 865–868.

Dickson, R.R., 1984. Eurasian snow cover versus Indian monsoon rainfall—an extension of the Hahn-Shukla results. Journal of Climatology and Applied Meteorology 23, 171–173.

Easterbrook, D.J., Pierce, K., Gosse, J.C., Gillespie, A., Evenson, E.B., Hamblin, K., 2003. Quaternary geology of the western United States. In: Easterbrook, D.J. (Ed.), Quaternary Geology of the United States. Geological Society of America, Denver, pp. 19–80.

Finkel, R.C., Owen, L.A., Barnard, P.L., Caffee, M.W., 2003. Beryllium-10 dating of Mount Everest moraines indicates a strong monsoonal influence and glacial synchroneity throughout the Himalaya. Geology 31, 561–564.

Gibbons, A.B., Megeath, J.D., Pierce, K.L., 1984. Probability of moraine survival in a succession of glacial advances. Geology 12, 327–330.

Gillespie, A., Molnar, P., 1995. Asynchronous maximum advances of mountain and continental glaciers. Reviews of Geophysics 33, 311–364.

Gosse, J.C., Phillips, F.M., 2001. Terrestrial in situ cosmogenic nuclides: theory and application. Quaternary Science Reviews 20, 1475–1560.

Gosse, J.C., Evenson, E.B., Klein, J., Lawn, B., Middleton, R., 1995a. Precise cosmogenic ^{10}Be measurements in western North America: support for a global younger Dryas cooling event. Geology 23, 877–880.

Gosse, J.C., Klein, J., Evenson, E.B., Lawn, B., Middleton, R., 1995b. Beryllium-10 dating of the duration and retreat of the Last Pinedale glacial sequence. Science 268, 1329–1333.

Hahn, D.G., Shukla, J., 1976. An apparent relationship between Eurasian snow cover and Indian monsoon rainfall. Journal of Atmospheric Science 33, 2461–2462.

Kodrau, O.D., 1981. Climatic Atlas of Asia. World Meteorological Organisation (UNESCO), Geneva.

Kohl, C.P., Nishiizumi, K., 1992. Chemical isolation of quartz for measurement of in-situ-produced cosmogenic nuclides. Geochimica et Cosmochimica Acta 56, 3583–3587.

Kuhle, M., 1985. Glaciation Research in the Himalayas: a new ice age theory. Universitas 27, 281–294.

Kuhle, M., 1988. Geomorphological findings on the built-up of Pleistocene glaciation in Southern Tibet and on the problem of inland ice. GeoJournal 17, 457–512.

Kuhle, M., 1991. Observations supporting the Pleistocene inland glaciation of High Asia. GeoJournal 25, 131–231.

Kuhle, M., 1995. Glacial isostatic uplift of Tibet as a consequence of a former ice sheet. GeoJournal 37, 431–449.

Lal, D., 1991. Cosmic ray labeling of erosion surfaces: in situ nuclide production rates and erosion models. Earth and Planetary Science Letters 104, 429–439.

Lal, D., Peters, B., 1967. Cosmic ray produced radioactivity on the Earth. In: Flugge, S. (Ed.), Handbuch der Physik, vol. 4612, pp. 551–612.

Lehmkuhl, F., 1997. Late Pleistocene, Late-Glacial and Holocene glacier advances on the Tibetan Plateau. Quaternary International 38/39, 77–83.

Lehmkuhl, F., Klinge, M., Lang, A., 2002. Late Quaternary glacier advances, lake level fluctuations and aeolian sedimentation in Southern Tibet. Zeitschrift für Geomorphologie 126, 183–218.

Meriaux, A.-S., Ryerson, F.J., Tapponnier, P., Van der Woerd, J., Finkel, R.C., Xu, X., Xu, Z., Caffee, M.W., 2004. Rapid slip along the central Altyn Tagh Fault: morphochronologic evidence from Cherchen He and Sulamu Tagh. Journal of Geophysical Research 109, B06401.

Molnar, P., England, P., 1990. Late Cenozoic uplift of mountain ranges and global climatic change: chicken or egg? Nature 346, 29–34.

Owen, L.A., Benn, D.I., 2005. Equilibrium-line altitudes of the Last Glacial Maximum for the Himalaya and Tibet: an assessment and evaluation of methods and results. Quaternary International, in press.

Owen, L.A., Lehmkuhl, F. (Eds.), 2000. Late Quaternary glaciation and palaeoclimate of the Tibetan Plateau and bordering mountains. Quaternary International 65/66, 212pp.

Owen, L.A., Zhou, S. (Eds.), 2002. Glaciation in Monsoon Asia, Quaternary International 97–98 179pp.

Owen, L.A., Gualtieri, L., Finkel, R.C., Caffee, M.W., Benn, D.I., Sharma, M.C., 2001. Cosmogenic radionuclide dating of glacial landforms in the Lahul Himalaya, Northern India: defining the timing of Late Quaternary glaciation. Journal of Quaternary Science 16, 555–563.

Owen, L.A., Finkel, R.C., Caffee, M.W., Gualtieri, L., 2002a. Timing of multiple glaciations during the Late Quaternary in the Hunza Valley, Karakoram Mountains, Northern Pakistan: defined by cosmogenic radionuclide dating of moraines. Geological Society of America Bulletin 114, 593–604.

Owen, L.A., Finkel, R.C., Caffee, M.W., 2002b. A note on the extent of glaciation in the Himalaya during the global Last Glacial Maximum. Quaternary Science Reviews 21, 147–157.

Owen, L.A., Kamp, U., Spencer, J.Q., Haserodt, K., 2002c. Timing and style of Late Quaternary glaciation in the eastern Hindu Kush, Chitral, northern Pakistan: a review and revision of the glacial chronology based on new optically stimulated luminescence dating. Quaternary International 97–98, 41–56.

Owen, L.A., Teller, J.T., Rutter, N.W., 2002d. Glaciation and reorganization of Asia's network of drainage. Global and Planetary Change 30, 289–374.

Owen, L.A., Spencer, J.Q., Ma, H., Barnard, P.L., Derbyshire, E., Finkel, R.C., Caffee, M.W., Zeng Yong, N., 2003a. Timing of Late Quaternary glaciation along the southwestern slopes of the Qilian Shan. Boreas 32, 281–291.

Owen, L.A., Ma, H., Derbyshire, E., Spencer, J.Q., Barnard, P.L., Zeng Yong Nian, Finkel, R.C., Caffee, M.W., 2003b. The timing and style of Late Quaternary glaciation in the La Ji Mountains, NE Tibet: evidence for restricted glaciation during the latter part of the Last Glacial. Zeitschrift für Geomorphologie 130, 263–276.

Owen, L.A., Finkel, R.C., Ma, H., Spencer, J.Q., Derbyshire, E., Barnard, P.L., Caffee, M.W., 2003c. Timing and style of Late Quaternary glaciations in NE Tibet. Geological Society of America Bulletin 115, 1356–1364.

Phillips, W.M., Sloan, V.F., Shroder, J.F., Sharma, P., Clarke, M.L., Rendell, H.M., 2000. Asynchronous glaciation at Nanga Parbat, northwestern Himalaya Mountains, Pakistan. Geology 28, 431–434.

Prell, W.L., Kutzbach, J.F., 1992. Sensitivity of the Indian monsoon to forcing parameters and implications for its evolution. Nature 360, 647–652.

Pu, J.-C., Su, Z., Yao, T.-D., Xie, Z.-C., 1998. Mass balance on Xiao Dongkemadi Glacier and Hailuoguo Glacier. Journal of Glaciology and Geocryology 12, 408–412.

Putkonen, J., Swanson, T., 2003. Accuracy of cosmogenic ages for moraines. Quaternary Research 59, 255–261.

Richards, B.W.M., Benn, D.I., Owen, L.A., Rhodes, E.J., Spencer, J.Q., 2000a. Timing of Late Quaternary glaciations south of Mount Everest in the Khumbu Himal, Nepal. Geological Society of American Bulletin 112, 1621–1632.

Richards, B.W., Owen, L.A., Rhodes, E.J., 2000b. Timing of Late Quaternary glaciations in the Himalayas of northern Pakistan. Journal of Quaternary Science 15, 283–297.

Ruddiman, W.F., Kutzbach, J.E., 1989. Forcing of Late Cenozoic Northern Hemisphere climate by plateau uplift in southern Asia and the America west. Journal of Geophysical Research 94, 409.

Schäfer, J.M., Tschudi, S., Zhao, Z., Wu, X., Ivy-Ochs, S., Wieler, R., Baur, H., Kubik, P.W., Schluchter, 2001. The limited influence of glaciations in Tibet on global climate over the past 170000 yr. Earth and Planetary Science Letters 6069, 1–11.

Sharma, M.C., Owen, L.A., 1996. Quaternary glacial history of the Garhwal Himalaya, India. Quaternary Science Reviews 15, 335–365.

Shi, Y., 2002. Characteristics of late Quaternary monsoonal glaciation on the Tibetan Plateau and in East Asia. Quaternary International 97–98, 79–91.

Shi, Y., Ge, Y., Xiaodong, L., Bingyuan, L., Tandong, Y., 2001. Reconstruction of the 30–40 ka BP enhanced Indian monsoon climate based on geological records from the Tibetan Plateau. Palaeogeography, Palaeoclimatology, Palaeoecology 169, 69–83.

Shiraiwa, T., 1993. Glacier fluctuations and cryogenic environments in the Langtang Valley, Nepal Himalaya. Contributions from the Institute of Low Temperature Science. The Institute of Low Temperature Sciences. Hokkaido University, Sapporo, Japan 98pp.

Sirocko, F., Sarnthein, M., Lange, H., Mayayewski, P.A., 1991. Atmospheric summer circulation and coastal upwelling in the Arabian Sea during the Holocene and the Last Glaciation. Quaternary Research 36, 72–93.

Soman, M.K., Slingo, J., 1997. Sensitivity of the Asian summer monsoon to aspects of sea-surface-temperature anomalies in the tropical Pacific Ocean. Quarterly Journal of the Royal Meteorological Society 123, 309–336.

Stone, J.O., 2000. Air pressure and cosmogenic isotope production. Journal of Geophysical Research 105, 23,753–23,759.

Su, Z., Shi, Y., 2002. Response of monsoonal temperate glaciers to global warming since the Little Ice Age. Quaternary International 97/98, 123–131.

Thomas, A., 1997. The climate of the Gongga Shan Range, Sichuan Province, PR China. Arctic and Alpine Research 29, 226–232.

Thompson, L.G., Thompson, E.M., Davies, M.E., Bolzn, J.F., Dai, J., Gunderstrup, N., Wu, X., Klein, L., Xie, Z., 1989. Holocene-Late Pleistocene climatic ice core records from the Qinghai-Tibet Plateau. Science 246, 474–477.

Thompson, L.G., Yao, T., Davis, M.E., Henderson, K.A., Mosley-Thompson, E., Lin, P.-N., Beer, J., Synal, H.A., Cole-Dai, J., Bolzan, J.F., 1997. Tropical climate instability: the Last Glacial Cycle from a Qinghai-Tibetan Ice Core. Science 276, 1821–1825.

Tsukamoto, S., Asahi, K., Watanabe, T., Rink, W.J., 2002. Timing of past glaciations in Kanchenjunga Himal, Nepal by optically stimulated luminescence dating of tills. Quaternary International 97/98, 57–67.

Wake, C.P., Mayewski, P.A., Dahe, Q., Qinzhao, Y., Sichang, K., Whitlow, S., Meeker, L.D., 2001. Changes in atmospheric circulation over the south-eastern Tibetan Plateau over the last two centuries from a Himalayan ice core. PAGES News 9, 14–16.

Winograd, I.J., Landwehr, J.M., Ludwig, K.R., Coplen, T.B., Riggs, A.C., 1997. Duration and structure of the past four interglacials. Quaternary Research 48, 141–154.

Yi, C., Li, X., Qu, J., 2002. Quaternary glaciation of Puruogangri-the largest modern ice field in Tibet. Quaternary International 97/98, 111–123.

Zech, W., Glaser, B., Abramowski, U., Dittman, C., Kubik, P.W., 2003. Reconstruction of the Late Quaternary Glaciation of the Macha Khola valley (Gorkha Himal, Nepal) using relative and absolute (^{14}C, ^{10}Be, dendrochronology) dating techniques. Quaternary Science Reviews 22, 2253–2265.

Zhao, H., Moore, G.W.K., 2004. On the relationship between Tibetan snow cover, the Tibetan plateau monsoon and the Indian summer monsoon. Geophysical Research Letters 31, L14204.

Zheng, B., 1989. The influence of Himalayan uplift on the development of Quaternary glaciers. Zietschrift für Geomorphologie 76, 89–115.

Zheng, B., 1997. Glacier variation in the monsoon maritime glacial region since the last glaciation on the Qinghai-Xizang (Tibetan) Plateau. In: The Changing Face of East Asia During the Tertiary and Quaternary. Center of Asian Studies, The University of Hong Kong, pp. 103–112.

Zheng, B. Jiao, K., 1991. Quaternary glaciations and periglaciations in the Qinghai-Xizang (Tibetan) Plateau. Excursion Guidebook XI, INQUA 1991, XIII International Congress, Beijing, 54pp.

Zreda, M.G., Phillips, F.M., 1995. Insights into alpine moraine development from cosmogenic ^{36}Cl buildup dating. Geomorphology 14, 149–156.